ACCELERON AEROSPACE JOURNAL (AAJ)
E-ISSN: 2583-9942 (Online) | Accessible at www.acceleron.org.in
Volume 5, Issue 4, (pp.1477-1515)
Article ID: AAJ.11.2106-2557
Research Paper
https://doi.org/10.61359/11.2106-2557

Conceptual Design and Aerodynamic Analysis of Medium Altitude Long Endurance VTOL Fixed wing UAV

Karthik Rajendran*

Senior Engineer Drone Solutions, Mistral Solutions Private Limited, Bangalore, Karnataka, India.

Abstract: This paper presents the conceptual design and multidisciplinary analysis of a Medium-Altitude Long-Endurance (MALE) Unmanned Aerial Vehicle (UAV) featuring a hybrid Vertical Take-Off and Landing (VTOL) and fixed-wing configuration. The design is driven by demanding mission requirements, including a 650 kg maximum take-off weight, a 100 kg payload capacity, a 200 km operational range, and an endurance of 10 hours at altitudes up to 7000 meters. The proposed twin-boom aircraft integrates an eight-rotor electric VTOL system for vertical flight and a conventional internal combustion engine (Rotax 914 ULF) for efficient forward cruise. The design process followed a systematic approach, beginning with initial sizing and weight estimation using empirical relations from Raymer's methodology, which established a baseline weight distribution. Constraint analysis identified the VTOL-to-cruise transition phase as the most critical, governing the thrust-to-weight ratio and wing loading. Aerodynamic design focused on the high-lift S1223 airfoil, with performance analyzed using XFLR5 and OpenVSP software to optimize the lift-to-drag ratio. Stability and control analysis were conducted to determine the optimal tail arm length of 3.85 meters, ensuring longitudinal and lateral stability, with the vertical stabilizer airfoil selection (NACA 0020) proving crucial for directional stability. Key results demonstrate a feasible design with an empty weight of 352 kg, a fuel weight of 185 kg, and a calculated cruise power requirement of 26 kW. The VTOL system requires a peak power of approximately 233 kW, met by eight 30 kW electric motors. The study concludes that the proposed VTOL fixed-wing UAV successfully balances the competing demands of vertical flight capability and long-endurance cruise performance. The insights and methodologies presented provide a robust foundation for future detailed design, prototyping, and flight testing of advanced hybrid UAVs.

Table of Contents

1. Introduction

Unmanned Aerial Vehicles (UAVs) have emerged as transformative tools in a wide range of applications, including surveillance, cargo delivery, disaster management, and environmental monitoring. Among the various configurations of UAVs, Vertical Take-Off and Landing (VTOL) fixed-wing UAVs have gained significant attention due to their unique ability to combine the efficiency of fixed-wing aircraft with the versatility of rotary-wing systems. VTOL capability allows these UAVs to operate in confined spaces without the need for runways, making them ideal for missions in urban environments, remote areas, or onboard ships. However, designing a VTOL fixed-wing UAV involves addressing complex challenges, including aerodynamic efficiency, propulsion system integration, and transition dynamics between hover and cruise phases. This paper presents the conceptual design of a VTOL fixed-wing UAV, aimed at achieving a balance between VTOL capability and long-endurance cruise performance. The design is driven by mission requirements such as a payload capacity of 100 kg, a range of 200 km, and an endurance of 10 hours, with the ability to operate at altitudes of up to 7000 meters above mean sea level (AMSL). The UAV is intended for applications such as persistent surveillance, cargo delivery, and search-and-rescue operations, where the combination of VTOL flexibility and fixed-wing efficiency is critical. The conceptual design

*Senior Engineer Drone Solutions, Mistral Solutions Private Limited, Bangalore, Karnataka, India. **Corresponding Author:** karthikdrt@gmail.com.
Article History: Received: 24-Sep-2025 || Revised: 22-Oct-2025 || Accepted: 22-Oct-2025 || Published Online: 30-Oct-2025.

process involves a multidisciplinary approach, integrating aerodynamics, propulsion, structural design, and performance analysis. Key considerations include the selection of an appropriate VTOL propulsion system (e.g., tiltrotor, tilt-wing, or hybrid configurations), optimization of the wing and fuselage geometry for aerodynamic efficiency and ensuring structural integrity under the diverse loads encountered during VTOL, transition, and cruise phases. Additionally, the design must address the challenges of weight management and energy efficiency, particularly in the context of hybrid or electric propulsion systems. This study contributes to the growing body of knowledge on VTOL fixed-wing UAVs by providing a systematic framework for conceptual design, supported by analytical calculations and performance simulations. The results of this work demonstrate the feasibility of a MALE VTOL fixed-wing UAV that meets the specified mission requirements while addressing the inherent trade-offs between VTOL capability and cruise efficiency. The insights gained from this study can serve as a foundation for future research, including detailed design, prototyping, and flight testing. The remainder of this paper is organized as follows: Section 2 outlines the Mission requirements and design objectives, Section 3 describes the Process Flow, Section 4 presents the Initial sizing and weight estimation, and Section 5 explains the Constraint Analysis, Section 6 depicts the Aerodynamic Design, Section 6 explores the Calculations for propulsion system selection, Section 7 explains the Conceptual Design and Weight distribution, Section 8 shows the graphical data of Stability and control and finally Section 9 concludes the results of the paper.

2. Mission Requirements

The conceptual design of the VTOL fixed-wing UAV is driven by a set of well-defined mission requirements, which ensure that the UAV meets the operational needs of its intended applications. These requirements are categorized into performance, payload, and operational constraints, as outlined below:

2.1 Performance Requirements

- **All-Up Weight (AUW):** The maximum takeoff weight of the UAV is 650 kg, inclusive of the payload, fuel, and onboard systems.
- **Range:** The UAV must achieve a minimum range of 200 km to support missions such as long-range surveillance, cargo delivery, or search-and-rescue operations.
- **Endurance:** The UAV is required to have an endurance of 10 hours, enabling persistent operations over extended periods.
- **Cruise Speed:** The UAV should maintain an efficient cruise speed of 30–50 m/s (108 km/h- 180km/hr) to balance aerodynamic performance and mission duration.
- **Altitude:** The operational altitude is specified as up to 7000 meters above mean sea level (AMSL), ensuring compatibility with high-altitude missions.
- **VTOL Capability:** The UAV must be capable of vertical take-off and landing (VTOL) to operate in confined or unprepared environments without the need for runways.

2.2 Payload Requirements

Maximum Payload Capacity: The UAV must accommodate a payload of up to 100 kg, which may include sensors, communication equipment, or cargo.

2.3 Operational Constraints

- **Environmental Conditions:** The UAV must operate reliably in a range of environmental conditions, including moderate wind speeds (up to 10 m/s) and temperatures ranging from -20°C to +45°C.
- **Launch and Recovery:** The UAV must support autonomous or semi-autonomous launch and recovery to minimize operational complexity.
- **Reliability and Redundancy:** The design must incorporate redundancy in critical systems (e.g., propulsion, avionics) to ensure safe operation in the event of component failure.
- **Regulatory Compliance:** The UAV must comply with relevant aviation regulations and standards for unmanned aircraft systems (UAS).

2.4 Design Drivers

- **Aerodynamic Efficiency:** The design must optimize the lift-to-drag ratio (L/D) to maximize range and endurance.
- **Propulsion System:** The propulsion system must support both VTOL and cruise phases, with sufficient thrust for hover and efficient power consumption for cruise.
- **Structural Integrity:** The airframe must be lightweight yet robust enough to withstand the loads encountered during VTOL, transition, and cruise.

Acceleron Aerospace Journal || AAJ.11.2106-2557
Volume 5, Issue 4, pp (1477-1515)
E-ISSN- 2583-9942
https://dx.doi.org/10.61359/11.2106-2557

- **Energy Management:** For electric or hybrid propulsion systems, the design must ensure efficient energy utilization to meet the endurance requirement.

2.5 Mission Scenarios

The UAV is designed to support a variety of mission scenarios, including:

- **Surveillance and Reconnaissance:** Long-endurance monitoring of remote or inaccessible areas.
- **Cargo Delivery:** Transport of supplies or equipment to remote locations.
- **Search and Rescue:** Locating and assisting individuals in disaster-stricken or hard-to-reach areas.
- **Environmental Monitoring:** Collecting data on atmospheric conditions, wildlife, or natural resources.

These mission requirements serve as the foundation for the conceptual design process, guiding the selection of key parameters such as wing area, propulsion system, and structural configuration. The subsequent sections of this paper detail the design methodology and analysis used to meet these requirements.

3. Process Flow / Methodical Approach

The conceptual design of the MALE VTOL fixed-wing UAV follows a structured and iterative process, ensuring that all mission requirements are met while addressing the inherent challenges of integrating VTOL capability with fixed-wing efficiency. The methodology is divided into the following key steps:

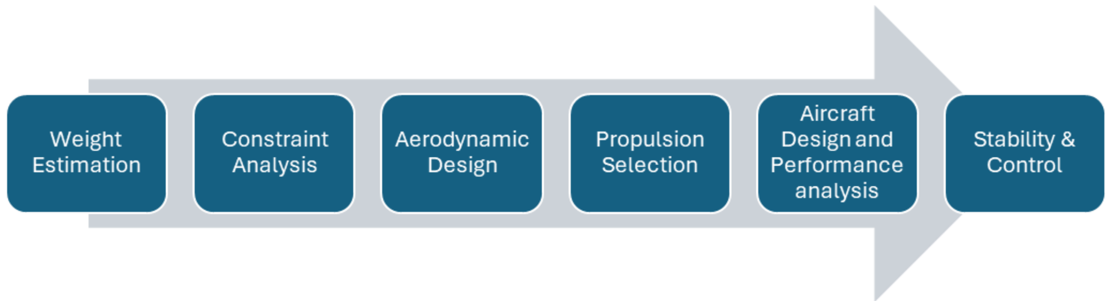

Figure 1 - Process Flow

3.1. Weight Estimation

Using empirical formulas (like those from Raymer's book) and mission requirements (payload, range, endurance), the team calculates the total take-off weight and then breaks it down into the weight of the structure (empty weight), the fuel, and the payload. The overall weight is the most fundamental parameter. It influences almost every other aspect of the design, from the size of the wing to the power of the engine.

3.2. Constraint Analysis

Analyzing different flight conditions (like take-off, climb, cruise, turn, and in this case, the critical VTOL transition) to determine the required thrust-to-weight ratio (T/W) and wing loading (W/S). This creates a "design space" graph, and the point that satisfies all constraints is selected. This step ensures the aircraft can actually perform its mission.

3.3. Aerodynamic Design

Selecting an appropriate airfoil (the cross-sectional shape of the wing) and designing the wing geometry (span, chord, aspect ratio). This is analyzed using software like XFLR5 to predict lift, drag, and the critical Lift-to-Drag (L/D) ratio. With the wing loading (W/S) from the previous step, the wing can be designed. Good aerodynamics are crucial for achieving the required range and endurance.

3.4. Propulsion Selection

Calculating the power required for both cruise (efficient forward flight) and VTOL (high-power hover). Based on these calculations, specific components are selected—internal combustion engine for cruise and eight electric motors for VTOL. The propulsion system can be selected only once we know how much power is needed (from constraint analysis and aerodynamic drag calculations) and how much the aircraft weighs.

3.5. Aircraft Design and Performance Analysis

Using CAD software (like OpenVSP), the team integrates all the previously designed components: fuselage, wing, tail, propulsion systems into a complete aircraft. This model is then analyzed to verify performance metrics like cruise speed, power required, and to ensure the weight distribution is correct. This is the integration phase where all the individual components (wing, engine, etc.) are brought together to see how they work as a whole system.

3.6. Stability & Control

Analyzing the aircraft's response to pitch, roll, and yaw. This includes checking the longitudinal stability (pitching moments) and lateral/directional stability (rolling and yawing moments due to sideslip), often by iterating on the size and position of the tail surfaces. Stability is checked on a nearly complete design. The geometry from the 3D model is used to calculate stability derivatives. If the aircraft is unstable, the design (especially the tail) must be modified and the process iterated.

4. Initial Sizing and Weight Estimation

Objective: Estimate the gross weight, empty weight, and fuel/battery weight using empirical equations and historical data.

Steps:

- Calculate the gross weight ($\boldsymbol{W_0}$) based on payload and mission requirements.
- Estimate the empty weight ($\boldsymbol{W_e}$) as a fraction of the gross weight.
- Calculate the fuel or battery weight ($\boldsymbol{W_{fuel}}$) based on endurance and propulsion system efficiency.

4.1 Gross Weight (W_0)

The gross weight is the total weight of the UAV at takeoff, which includes:

- Empty Weight (W_e)
- Payload Weight ($W_{payload}$)
- Fuel Weight (W_{fuel})

For your UAV:

$$W_0 = W_{payload} + W_{fuel} + W_e$$

$$W_0 = W_{payload} + \left(\frac{W_{fuel}}{W_0}\right) W_0 + \left(\frac{W_e}{W_0}\right) W_0$$

$$W_0 = \frac{W_{payload}}{1 - \left(\frac{W_{fuel}}{W_0}\right) - \left(\frac{W_e}{W_0}\right)}$$

4.2 Empty Weight Fraction ($\frac{W_e}{W_0}$)

According to the Book "Aircraft Design- A Conceptual Approach" by Raymer provides empirical equations to estimate the empty weight fraction based on the type of aircraft; the empty weight fraction can be estimated as:

$$\frac{W_e}{W_0} = A * W_0^C * K_{vs}$$

Where:

- A and C are constants based on aircraft type.
- $\boldsymbol{K_{vs}}$ is the variable sweep factor (1.0 for fixed-wing).

For a UAV – Recce and UCAVs, Raymer suggests:

- $A = 1.53$
- $C = -0.16$

Thus:

$$\frac{W_e}{W_0} = 1.53 * (650)^{-0.16} = 0.542$$

Acceleron Aerospace Journal || AAJ.11.2106-2557
Volume 5, Issue 4, pp (1477-1515)
E-ISSN- 2583-9942
https://dx.doi.org/10.61359/11.2106-2557

4.3 Fuel Weight Fraction ($\frac{W_{fuel}}{W_0}$)

$$W_{fuel} = W_{mission\ fuel}$$

The $W_{mission\ fuel}$ depends upon

- Type of Mission
- Aircraft Aerodynamics
- Engine SFC

Assumption

- Fuel used in each mission segment is proportional to a/c weight during mission segment
- Hence $\boldsymbol{W_{fuel}}$ is independent of the aircraft weight

Fuel Weight can be calculated based on Breguet Endurance and Range equation for a simple mission profile which is stated below:

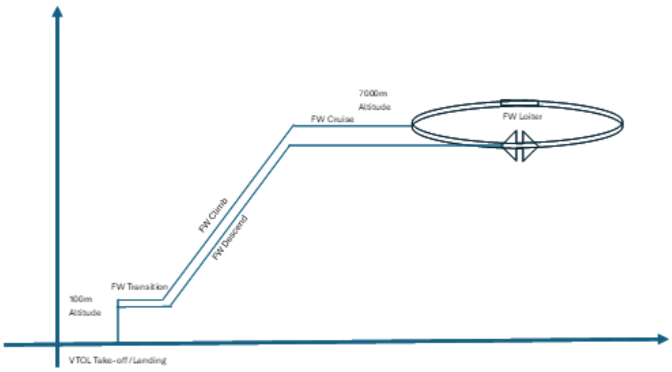

Figure 2 - Mission Profile

The mission consists of:

(The VTOL Take-off and landing will be neglected as this will be taken care by the VTOL propulsion system which is electric.)

1. **Transition & Climb** → Up to 7000m AMSL
2. **Cruise** → 200 km
3. **Loiter** → At destination
4. **Return** → Back to base

The total fuel fraction is given by:

$$\frac{W_{fuel}}{W_0} = 1 - \frac{W_5}{W_0} \quad \text{where } \frac{W_5}{W_0} = \frac{W_5}{W_4} * \frac{W_4}{W_3} * \frac{W_3}{W_2} * \frac{W_2}{W_1} * \frac{W_1}{W_0}$$

Each term represents the weight fraction for a specific phase:

- $\frac{W_1}{W_0}$ = Takeoff (Neglected as its electric VTOL)
- $\frac{W_2}{W_1}$ = Transition & Climb fuel fraction
- $\frac{W_3}{W_2}$ = Outbound cruise fuel fraction
- $\frac{W_4}{W_3}$ = Loiter fuel fraction
- $\frac{W_5}{W_4}$ = Return cruise fuel fraction

The Breguet Range Equation is a fundamental formula used in aviation to estimate the range of an aircraft during Various stages of flight. The equation is particularly useful for determining the fuel fraction required for cruise. The general form of the Breguet Range Equation for propeller aircraft is:

$$R = \frac{\eta * V}{C} * \frac{L}{D} * \ln \frac{W_{initial}}{W_{final}}$$

Where:

- R = Range (in kilometers)
- V = Velocity
- η = Propeller Efficiency
- C = Specific fuel consumption (in kg/kW-hr)
- $\frac{L}{D}$ = Lift-to-drag ratio (dimensionless)
- $W_{initial}$= Initial weight of the aircraft (including fuel, in kg)
- W_{final}= Final weight of the aircraft (after fuel burn, in kg),

Finally rewriting the Equation,

$$\frac{W_{initial}}{W_{final}} = e^{-\left(\frac{R*C}{\eta * V * (\frac{L}{D})}\right)}$$

The Fuel Fraction is,

$$Fuel\ Fraction = 1 - \frac{W_{initial}}{W_{final}} = 1 - e^{-\left(\frac{R*C}{\eta * V * (\frac{L}{D})}\right)}$$

Similarly, The Breguet's Endurance is also used which is as follows,

$$E = \frac{\eta}{C} * \frac{L}{D} * \ln \frac{W_{initial}}{W_{final}}$$

Where:

- E = Time (in hours)
- η = Propeller Efficiency (As our Aircraft is prop driven)
- C = Specific fuel consumption (kg/kW-hr)
- $\frac{L}{D}$ = Lift-to-drag ratio (dimensionless)
- $W_{initial}$= Initial weight of the aircraft (including fuel, in kg)
- W_{final}= Final weight of the aircraft (after fuel burn, in kg)

Key Notes: The Velocity (V) doesn't appear in endurance equation, because in loiter, the aircraft is staying in one location and fuel consumption is tied to how long it can stay airborne per unit fuel.

The power required for loiter is:

$$P_{loiter} = \frac{D}{\eta}$$

Since, $D = \frac{W}{L/D}$, we get:

$$P_{loiter} = \frac{W}{\left(\frac{L}{D}\right) * \eta}$$

Unlike cruise, time (endurance) is independent of velocity, so it does not appear in the equation.

Thus, only propeller efficiency appears in the loiter equation because fuel consumption depends on how efficiently power is used per unit time.

Acceleron Aerospace Journal || AAJ.11.2106-2557
Volume 5, Issue 4, pp (1477-1515)
E-ISSN- 2583-9942
https://dx.doi.org/10.61359/11.2106-2557

Check for updates

The Fuel Fraction is,

$$Fuel\ Fraction = 1 - \frac{W_{initial}}{W_{final}} = 1 - e^{-\left(\frac{E*C}{\eta*\left(\frac{L}{D}\right)}\right)}$$

Key Notes: The equation assumes steady-level flight with constant specific fuel consumption and lift-to-drag ratio.

Initial Aerodynamic Analysis:

To obtain an optimum L/D, a python code was created, which calculated the best Cl, Cd and L/D by giving following inputs, based on various iterations, the following values arrived.

Table 1- Design parameters for initial aerodynamic analysis

S.no	Design Parameters	Values	Units	Remarks
1	Weight	650	Kg	
2.	Air density	0.589	Kg/m^3	
3.	Wing Span	10	m	
4.	Wing Chord	0.75	m	
5.	Co-Efficient of Drag	0.07		Assumed
6.	Airspeed	45	m/s	
7.	Oswald Efficiency	0.8		Assumed
8.	Aifoil Cl_Max	2.2		S1223 Airfoil was chosen
9.	Wing Sweep	0	Deg	
10	Viscosity	2.64e-5		

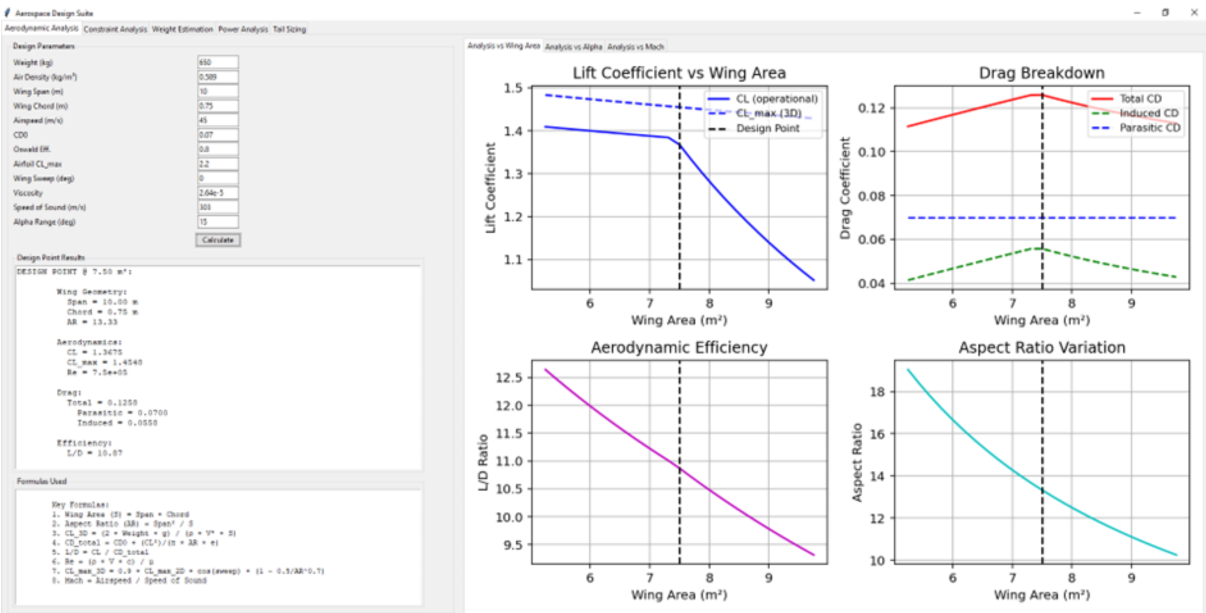

Figure 3 - Aerodynamic Performance Analyzer

Key Formula's Used:

1. $Wing\ Area = Span * Chord$
2. $Aspect\ Ratio(AR) = \frac{Span^2}{S}$
3. $CL_{3D} = \frac{2*Weight*g}{rho*V^2*S}$
4. $CD_{total} = CD_0 + \frac{CL^2}{Pi*AR*e}$
5. $L/D = (CL/CD\_total)$
6. $Re = \frac{rho*V*c}{mu}$
7. $CL_{max3D} = 0.9 * CL_{\max 2D} * Cos(Sweep) * (1 - \frac{0.5}{AR^{0.7}})$

With the Above values and formulas used, the Design point was calculated with respect Wing Area, Alpha and Mach.

Key Aspects of the Code:

1. **3D Correction Factors**:
   The script applies realistic 3D wing corrections that reduce the CL from the ideal 2D value:
   - 0.9 factor for 3D effects
   - cos(sweep) factor (though sweep = 0° in this case)
   - Aspect ratio reduction term $\left(1 - \frac{0.5}{AR^{0.7}}\right)$
2. **Safety Margin**:
   The script limits CL to 95% of CL_max, whereas the manual calculation didn't account for this.
3. **Induced Drag Consideration**:
   The script uses a more sophisticated calculation that accounts for how induced drag affects the achievable CL.

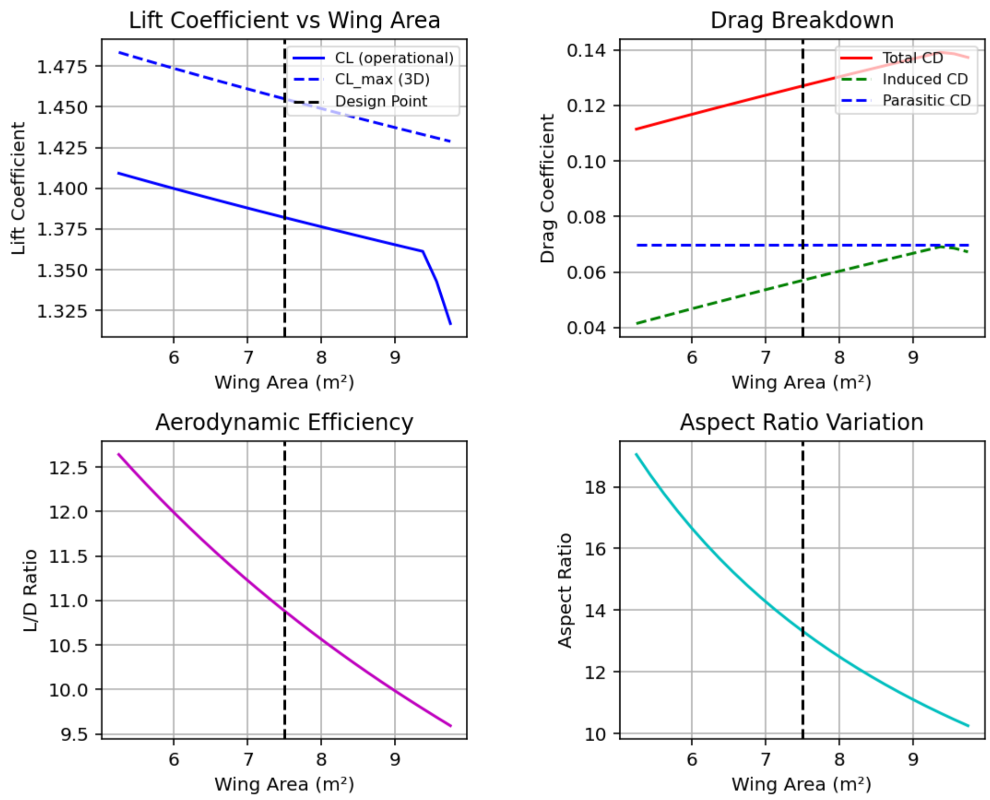

Figure 1 - Aerodynamic constants vs Wing Area

Volume 5, Issue 4, pp (1477-1515)
E-ISSN- 2583-9942
https://dx.doi.org/10.61359/11.2106-2557

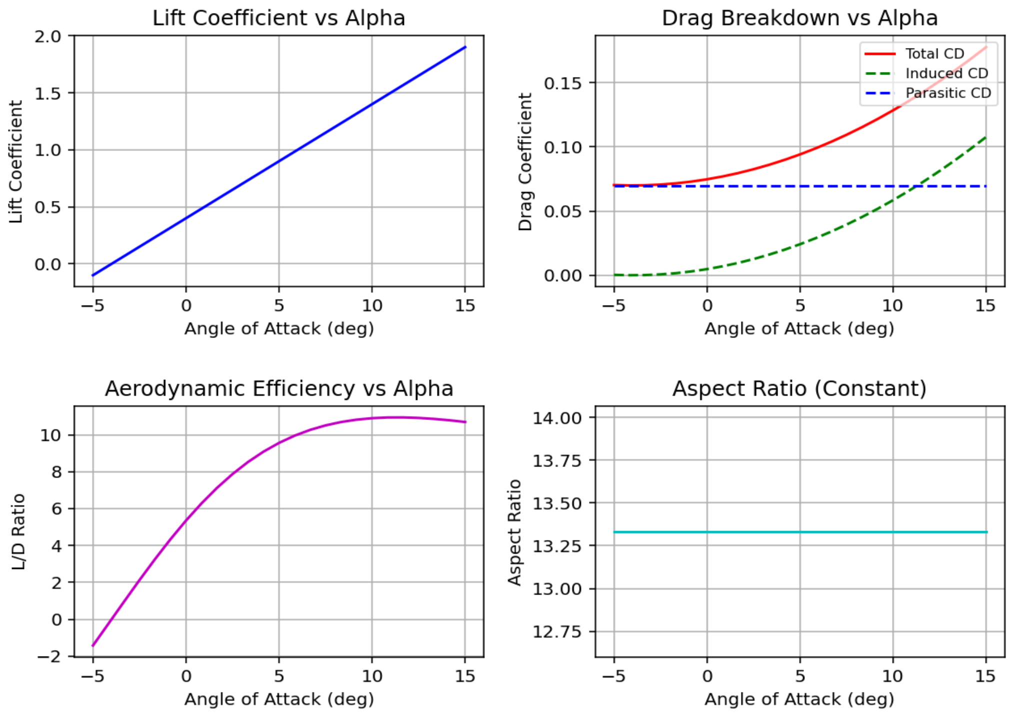

Figure 2 - Aerodynamic constants vs AoA

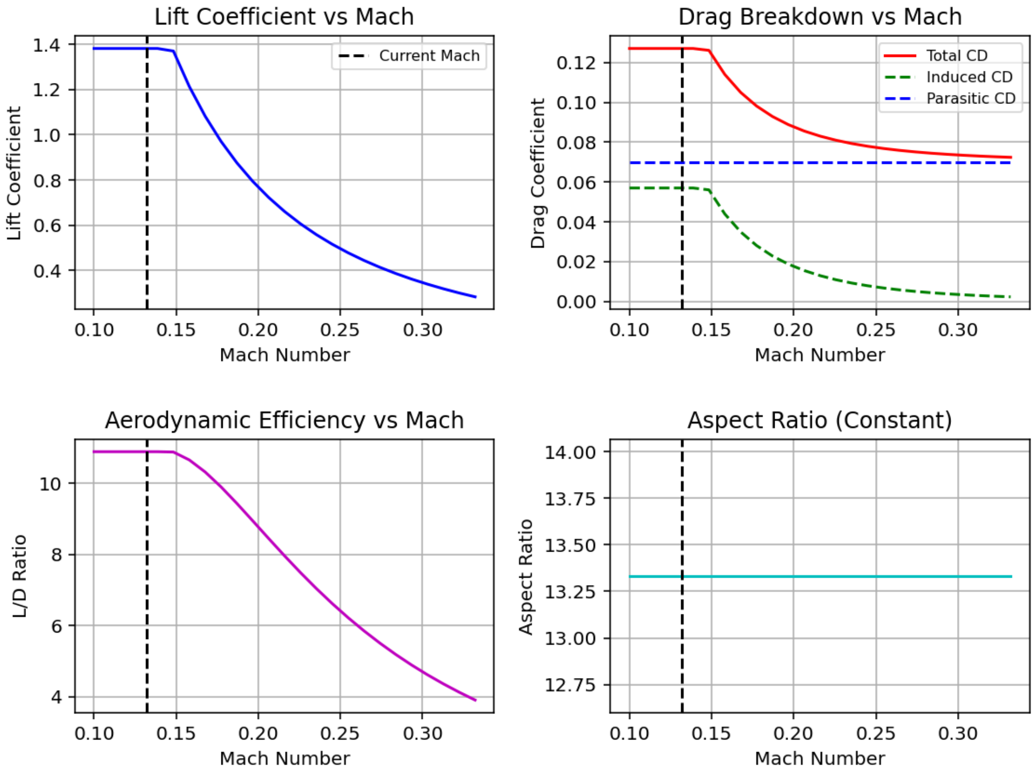

Figure 3 - Aerodynamic constants vs Mach

Final Design point Results:

Design Point Results

```
DESIGN POINT @ 7.50 m²:

        Wing Geometry:
          Span = 10.00 m
          Chord = 0.75 m
          AR = 13.33

        Aerodynamics:
          CL = 1.3675
          CL_max = 1.4548
          Re = 7.5e+05

        Drag:
          Total = 0.1258
            Parasitic = 0.0700
            Induced = 0.0558

        Efficiency:
          L/D = 10.87
```

Figure 4 - Final Design points

With the following results obtained, we will calculate the fuel fraction for each stage of the mission

1. MTOW (W_0) = 650 kg
2. Propeller-Driven Aircraft (As we are using an IC Engine which is apt for low-speed aircrafts)
3. Cruise Speed = 45 m/s (162 km/h) (Assumed Speed with reference to multiple other UAVs of this same weight spec)
4. Specific Fuel Consumption (SFC) = 0.3 kg/kW-hr
5. $\frac{L}{D}$ Ratio = 10.87
6. Propeller Efficiency (η) = 0.7
7. Altitude = 7000 m AMSL
8. Range = 200 km (one-way)
9. Loiter Time = 5 hours

A Python Code was created for this weight estimation as well, with formulas infused from Raymer's book.

Table 2 - Design parameters for initial weight analysis

S.no	Design Parameters	Values	Units	Remarks
1	Weight	650	Kg	
2.	Cruise Speed	45	m/s	
3.	SFC	0.3	Kg/kWh	Assumed
4.	L/D ratio	10.87		From the Previous findings
5.	Prop Efficiency	0.7		Assumed
6.	Cruise Range	200	Km	One way cruise
7.	Loiter Time	5	Hrs	
8.	Climb Fuel Factor	0.04		Assumed

Volume 5, Issue 4, pp (1477-1515)
E-ISSN- 2583-9942
https://dx.doi.org/10.61359/11.2106-2557

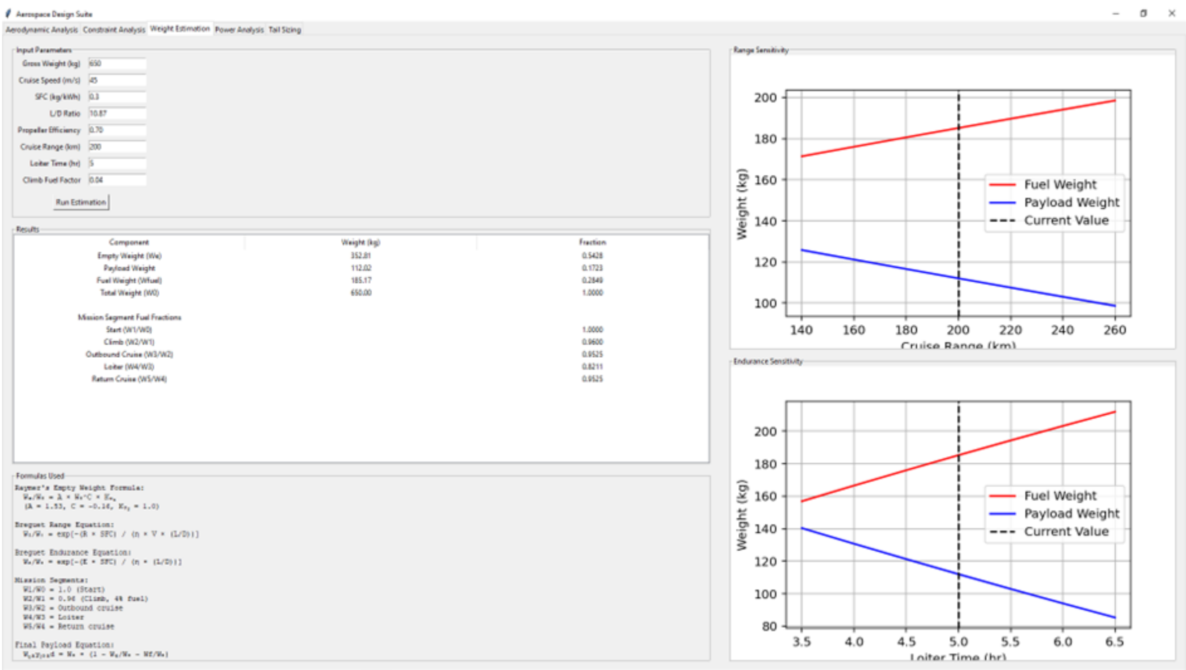

Figure 8 - Aircraft Weight Estimation Tool

Climb Fuel Fraction ($\frac{W_2}{W_1}$):

The Climb Fuel Factor is assumed to be 4% of total fuel which is 0.96

Cruise Fuel Fraction ($\frac{W_3}{W_2}$):

$$\frac{W_3}{W_2} = e^{-\left(\frac{R*C}{\eta*V*\left(\frac{L}{D}\right)}\right)} = e^{-\left(\frac{(200*1000)*0.3}{(0.70*45*3600)*(10.87)}\right)} = 0.9525$$

Loiter Fuel Fraction ($\frac{W_4}{W_3}$):

$$\frac{W_4}{W_3} = e^{-\left(\frac{E*C}{\eta*\left(\frac{L}{D}\right)}\right)} = e^{-\left(\frac{5*0.3}{(0.70)*(10.87)}\right)} = 0.8211$$

Return Cruise Fuel Fraction ($\frac{W_5}{W_4}$):

$$\frac{W_5}{W_4} = \textit{is as same as the outbound cruise}, \text{ So } \frac{W_5}{W_4} = 0.9525$$

So, the total Fuel Factor is as follows,

$$\frac{W_{fuel}}{W_0} = 1 - \frac{W_5}{W_0} \quad \text{where } \frac{W_5}{W_0} = \frac{W_5}{W_4} * \frac{W_4}{W_3} * \frac{W_3}{W_2} * \frac{W_2}{W_1} * \frac{W_1}{W_0}$$

$$\frac{W_5}{W_0} = 0.9525 * 0.8211 * 0.9525 * 0.96 = 0.7151$$

$$\frac{W_{fuel}}{W_0} = 1 - 0.7151 = 0.2849$$

4.4 Payload Weight Fraction (W_payload)

By substituting $\frac{W_{fuel}}{W_0}$ *and* $\frac{W_e}{W_0}$ in $W_0 = \frac{W_{payload}}{1-\left(\frac{W_{fuel}}{W_0}\right)-\left(\frac{W_e}{W_0}\right)}$, We Get,

$$650kg = \frac{W_{payload}}{1-(0.2849)-(0.5428)} = \frac{W_{payload}}{0.1723}$$

$$W_{payload} = 650 * 0.173 = 112\ kg$$

4.5 Final Weight Distribution

Finally, The Weight Estimation is given in the table below,

Table 3 - Weight Distribution

Weights	Value
W_{empty}	352.81 Kg
$W_{payload}$	112 Kg
W_{Fuel}	185.17 Kg
W_{total}	650kg

This is the Overall weight estimate where a 650Kg VTOL can fly up to 200Km range and loiter up to 5 Hours and come and land at the Take-off point with an overall endurance up to 10 hours. The Final Results from the python program and two graphs indicating the relation between Fuel and payload weight vs Cruise Range & Fuel and Payload weight vs Endurance.

Results

Component	Weight (kg)	Fraction
Empty Weight (We)	352.81	0.5428
Payload Weight	112.02	0.1723
Fuel Weight (Wfuel)	185.17	0.2849
Total Weight (W0)	650.00	1.0000
Mission Segment Fuel Fractions		
Start (W1/W0)		1.0000
Climb (W2/W1)		0.9600
Outbound Cruise (W3/W2)		0.9525
Loiter (W4/W3)		0.8211
Return Cruise (W5/W4)		0.9525

Figure 9 - Final Weight Estimation Result

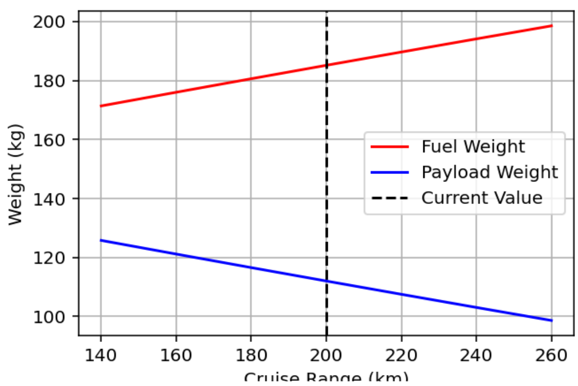

Figure 1 - Weight vs Cruise Range

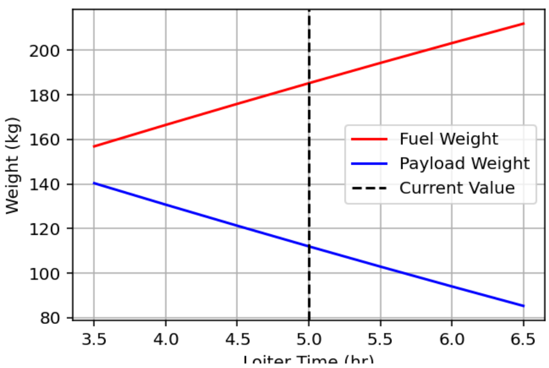

Figure 2 - Weight vs Loiter Time

Acceleron Aerospace Journal || AAJ.11.2106-2557
Volume 5, Issue 4, pp (1477-1515)
E-ISSN- 2583-9942
https://dx.doi.org/10.61359/11.2106-2557

5. Constraint Analysis

Constraint analysis is a crucial part of the conceptual and preliminary aircraft design process because it helps define the performance boundaries and ensures the aircraft can safely and effectively complete its mission.

Here the Constraint analysis is done for the Aircraft considering the flight parameters according to the mission which was seen above. The Following parameters were taken into consideration and special python Code was developed to Calculate the Design Constraint.

Table 4 - Parameters for Constraint Analysis

Parameter	Value
MTOW	650 kg
Cruise Speed (V_c)	45 m/s
Climb Speed (V_cl)	42 m/s
Climb Rate (R_c)	2.5 m/s
Stall Speed (V_s)	36.2 m/s
Airfoil CL_max	2.2
CD0	0.07
Wing Span	10 m
Wing Chord	0.75 m
Oswald Efficiency (e)	0.8
Bank Angle	20°
ρ_cruise	0.59 kg/m³
$\rho\_sea\ level$	1.225 kg/m³
g	9.81 m/s²

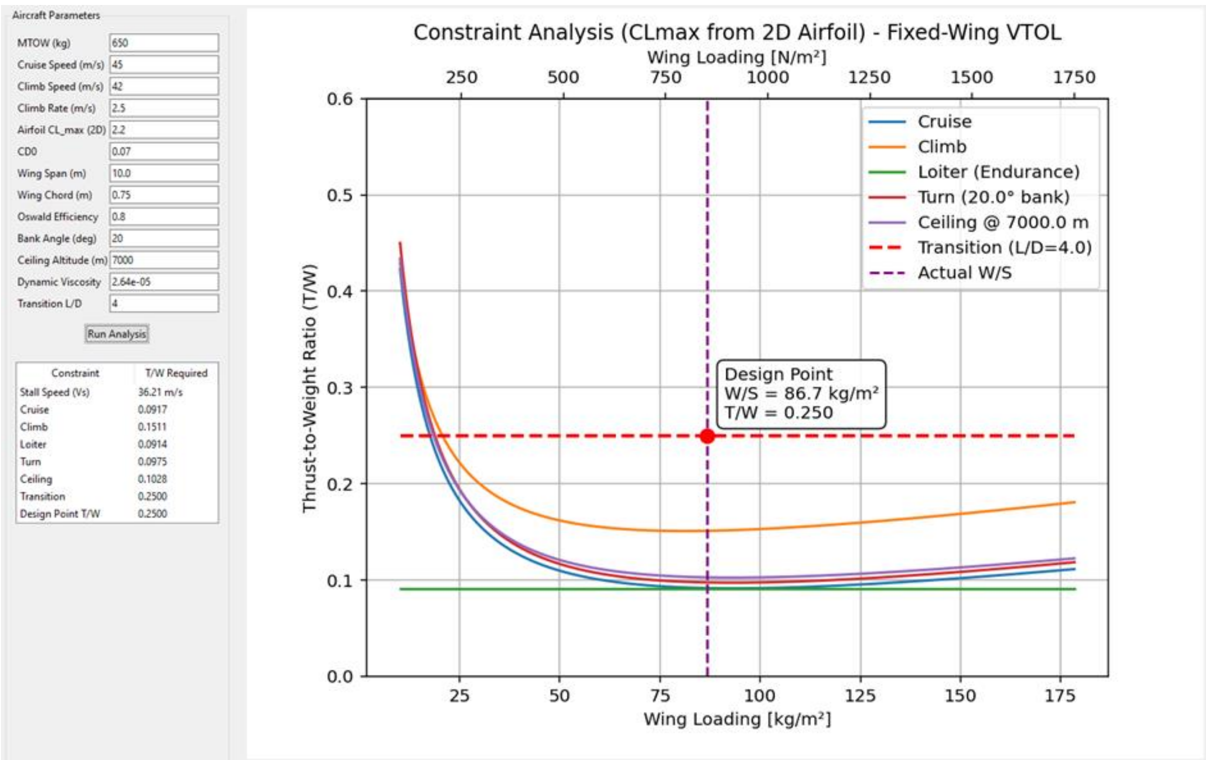

Figure 12 - UAV Constraint Analysis Tool

Summary of Constraints at W/S = 86.7 kg/m²

Constraint	T/W Required
Cruise	0.0917
Climb	0.1714
Loiter	0.0914
Banked Turn (20°)	0.0975
Transition	0.250
Ceiling	0.1028

Critical Constraint: Transition (T/W = 0.25) governs the design.

Constraint Analysis Summary

Critical Constraints:

- **Stall Limit**: 102.19 kg/m² (The design is safely below this)
- **Most Demanding Phase**: Transition (requires T/W = 0.25)
- **Design Point**: 86.70 kg/m² (T/W = 0.25)

6. Aerodynamic Design

Aerodynamic design plays a crucial role in aircraft development as it directly affects performance, efficiency, stability, and safety. A well-optimized aerodynamic shape minimizes drag and maximizes lift, improving fuel efficiency and allowing the aircraft to achieve longer endurance with less power consumption. The choice of airfoil, wing configuration, and overall shape determines cruise speed, range, and climb performance, ensuring the aircraft meets its mission requirements effectively.

6.1 Reynold's Number Calculation

For analysing air foil characteristics at 7000m AMSL, a typical operating Reynolds number is required

With the following inputs, the Reynold's Number:

1. **Airspeed (V)**: 45 m/s
2. **Chord Length (c)**: 0.75
3. **Air Density (*ρ*)**: At 7000 meters AMSL (cruise altitude), the air density is approximately 0.589 kg/m³ with 15°C Temperature Offset (from standard atmospheric tables).
4. **Dynamic Viscosity (*μ*)**: For air, μ ≈ 1.56e-05

$$Re = \frac{\rho * V * c}{\mu} = \frac{0.589 * 45 * 0.75}{1.56 * 10^{-5}} = \frac{17.67}{1.56 * 10^{-5}} \approx 1.13\ Million$$

So, the Airfoil characteristics must be analysed for 0.5 – 1.5 million Reynolds Number.

6.2 Airfoil Selection

For our Design we have chosen S1223 airfoils based on the already available aircraft and their designs which closely matches our requirements

The aerofoil is well-known and have been used in various aircraft, including UAVs. I'll provide a comparative analysis based on aerodynamic properties and typical applications

Acceleron Aerospace Journal || AAJ.11.2106-2557
Volume 5, Issue 4, pp (1477-1515)
E-ISSN- 2583-9942
https://dx.doi.org/10.61359/11.2106-2557

6.2.1 Parametric Table

Table 6 - S1223 Air foil Specifications

Parameter	**S1223**
Thickness	12.1%
Camber	High
Reynolds Range	100k – 1.5M
L/D Ratio	~120
Clmax	~2.3
Stall Behaviour	Gentle
Usage in UAVs	AeroVironment Raven

6.3 Wing Analysis on XFLR5 Software:

Based on this aerofoil, we have designed the wing in XFLR5 with the following assumptions:

1. Wingspan: 10m (This wingspan was taken from TATICAL HERON UAV which closely matches our requirements and design)
2. Chord length: 0.75m
3. MAC: 0.75m
4. Wing Area:7.5 m^2
5. Plane Mass: 650Kg
6. Wing Loading: 86.6 Kg/m^2
7. Aspect Ratio: 13.33
8. Taper Ratio: 1

The wing design:

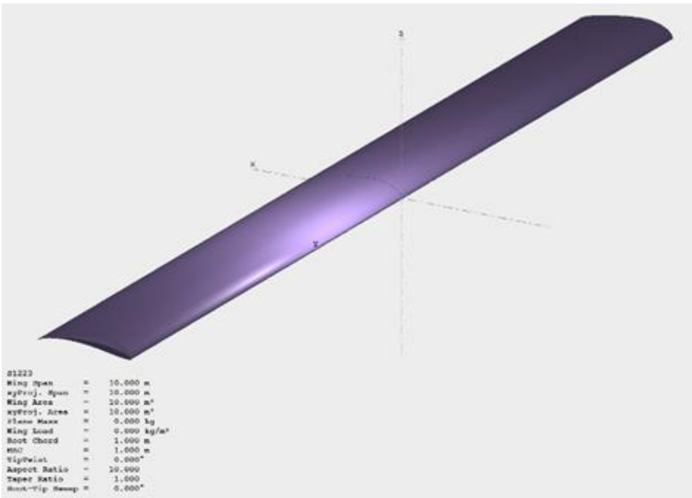

Figure 13 - Wing Design with S1223 Airfoil

The Analysis was done based on 3D Plane

3D Plane: 3D Plane Analysis in XFLR5 is a more advanced method that extends the capabilities of LLT by incorporating viscous effects and non-linear aerodynamics. It uses a panel method to solve the flow around the wing in three dimensions, providing more accurate results than LLT. based on these two analyses, the following Results were obtained

1. Cl vs Alpha	2. Cd vs Alpha	3. ClCD vs Alpha	4. Cl vs Cd

6.3.1 Comparative Diagram and Graphs

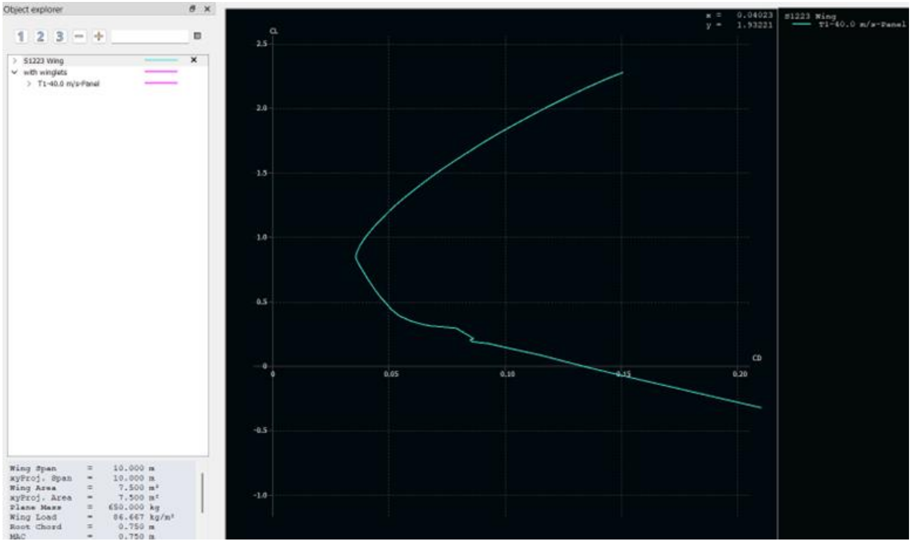

Figure 14 - S1223 Wing Analysis CL vs CD

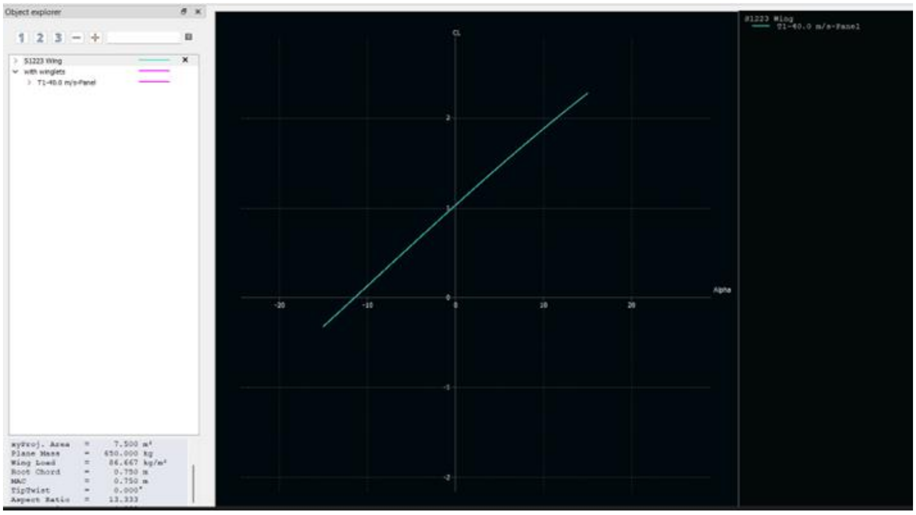

Figure 15 - S1223 Wing Analysis CL vs Alpha

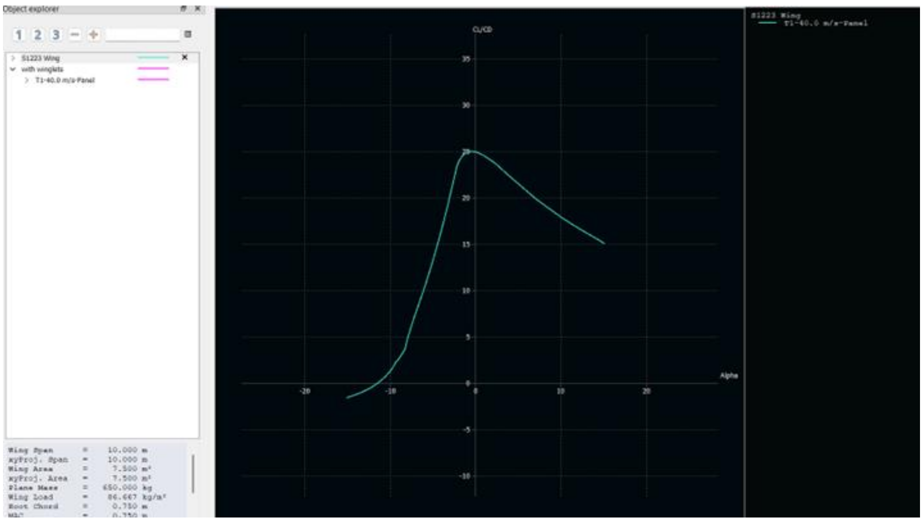

Figure 16 - S1223 Wing Analysis L/D vs Alpha

Acceleron Aerospace Journal || AAJ.11.2106-2557
Volume 5, Issue 4, pp (1477-1515)
E-ISSN- 2583-9942
https://dx.doi.org/10.61359/11.2106-2557

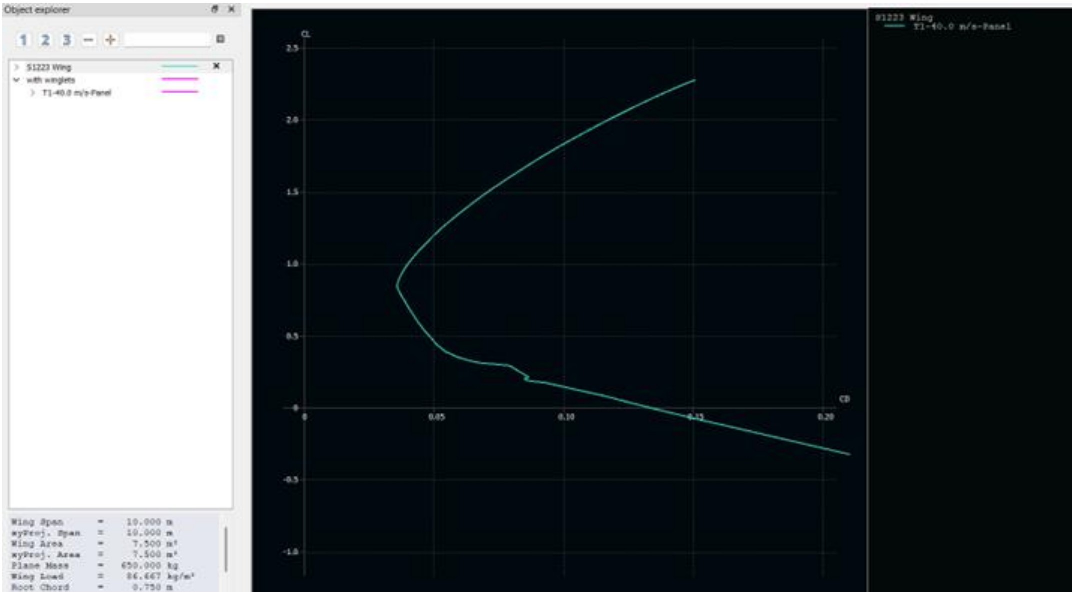

Figure 17 - S1223 Wing Analysis CL vs CD

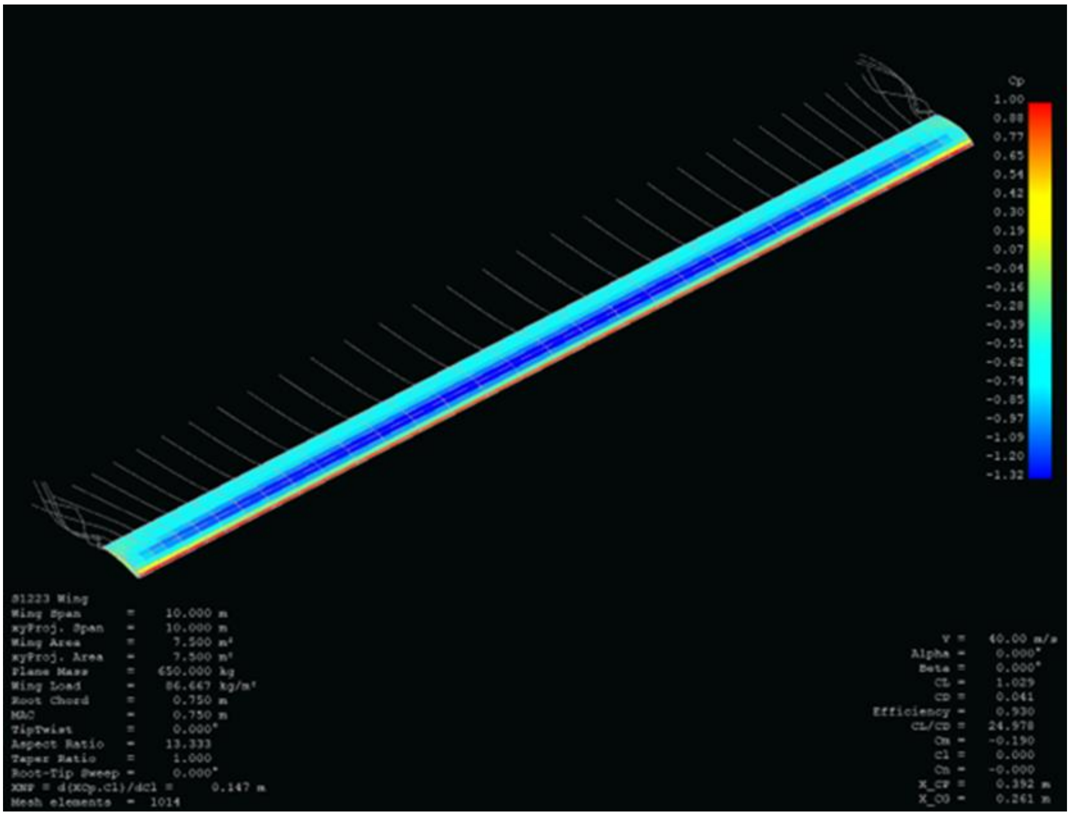

Figure 18 - Pressure Distribution at 0 Deg AOA

From the above data, we can see that the wing designed with S1223 Airfoil has a low drag and high L/D ratio. Also, the pressure distribution is even.

6.3.2 CLIMB Analysis

Further the AoA for climb will be calculated and analysis will be made for those angles. To calculate the required angle of attack (AoA) for the aircraft to climb from 100m to 7500m at a climb rate of 2.5 m/s(Assumed), we need to consider the climb performance of the aircraft. The angle of attack during climb is influenced by the climb rate, airspeed, and aerodynamic forces (lift and drag). Here's how we have approached the problem:

Climb Scenario

- **Climb Rate (V_y)**: 2.5 m/s (vertical velocity).
- **Airspeed (V)**: 45 m/s (given).
- **Altitude Change**: From 100m to 7000m (climb gradient is small, so we can assume constant air density and performance).
- S1223 Airfoil Properties:
  - Lift curve slope (C_Lα): 0.11 per degree
  - Zero-lift AoA (α_0): -3.5°

Climb Angle (θ)

$$\sin\theta = \frac{V_y}{V}$$

$$\theta = \sin^{-1}\frac{V_y}{V} = \sin^{-1}\left(\frac{2.5}{45}\right) = 3.18°$$

Adjust CL for Climb

For small θ (< 5°), $cos\theta \approx 1$, so:

$$C_{LClimb} = \frac{C_{LLevel}}{Cos\theta} = 1.3675\ (No\ Significant\ Changes)$$

Angle of Attack

$$\alpha = \frac{C_{Lclimb}}{C_{L\alpha}} + \alpha 0 = \frac{1.3675}{0.11} + (-3.5°) = 8.93°$$

Effective Angle of Attack (α_{eff})

$$\boldsymbol{\alpha_{eff}} = \boldsymbol{\alpha} - \theta = 8.93 - 3.58 = 5.35°$$

The **required angle of attack** to achieve the climb rate of 2.5 m/s is approximately 5.35°. This is the angle at which the airfoil must be set relative to the oncoming airflow to generate the necessary lift for the climb.

6.4 Fuselage Sizing

1. Fuselage Length

Raymer provides empirical relationships for fuselage length based on the type of aircraft. For UAVs and general aviation aircraft, the fuselage length is often proportional to the wingspan.

Raymer's Empirical Formula:

For general aviation aircraft, the fuselage length (L_{Fus}) can be estimated as:

$$L_{Fus} = \frac{wingspan}{length} ratio * Wingspan\ (\frac{wingspan}{length} ratio\ is\ taken\ from\ below\ table)$$

The design we propose here is like Heron UAVs Which have Twin Boom Configuration.

Acceleron Aerospace Journal || AAJ.11.2106-2557
Volume 5, Issue 4, pp (1477-1515)
E-ISSN- 2583-9942
https://dx.doi.org/10.61359/11.2106-2557

Table 7 - Comparison Table for Various UAV for wingspan to length ratio

UAV Model	Wingspan (m)	Overall Length (m)	Wingspan to length Ratio (W/L)	Configuration
Heron TP	26	14	0.53	Twin Boom tail, pusher
Heron	16.6	8.5	0.51	Twin Boom tail, pusher
Tactical Heron	10.6	7.3	0.68	Twin Boom tail, pusher
FH-95(Feihong)	12	7.9	0.65	Twin Boom tail, pusher
Mohajer-6	9.99	5.66	0.56	Twin Boom tail, pusher

For most MALE UAVs, the ratio of overall length to wingspan is approximately 0.5 to 0.6. So, For Our VTOL UAV we will consider 0.55 as well be integrating the VTOL motors in the boom (During Design phase, this may increase due to VTOL propeller Diameter constrains).

Calculation:

- **Wingspan**: 10m
- **Fuselage Length**:

$$L_{Fus} = 0.55 * 10 = 5.5m$$

6.5 Tail Sizing

Raymer provides detailed methods for sizing the horizontal and vertical stabilizers using tail volume coefficients. These coefficients are based on the aircraft's wing geometry and desired stability characteristics.

Twin Boom Configuration:

The twin boom tail configuration offers several advantages for this design. It provides ample propeller clearance, avoiding interference with VTOL rotors during hover and transition, while twin vertical stabilizers enhance yaw stability and control, crucial for crosswind conditions and maneuvering. The design improves structural strength, distributing loads evenly to handle VTOL stresses, and offers space between the booms for payload or sensor integration. Additionally, it reduces interference drag, optimizing aerodynamic efficiency for forward flight, making it a robust and versatile choice for VTOL operations.

6.5.1 Horizontal Stabilizer Sizing

The horizontal tail volume coefficient (V_h) is given by:

$$V_h = \frac{S_h * L_h}{S * MAC}$$

Where:

- $\boldsymbol{S_h}$ = Horizontal stabilizer area.
- $\boldsymbol{L_h}$ = Tail arm (distance from the wing's aerodynamic centre to the tail's aerodynamic centre).
- S = Wing area.
- MAC = Mean aerodynamic chord.

Tail Arm (L_h):

$$\boldsymbol{L_h} = 0.7 * Fuselage\ Length = 0.7 * 5.5 = 3.85m$$

As we need to integrate the VTOL propulsion System, The Tail Arm considered is at least 70% of the Fuselage length which is quite large than the default value of 50-60%.

For UAVs and general aviation aircraft, V_h typically ranges from 0.35 to 0.7.

Using $\boldsymbol{V_h}$**=** 1.1, This is because we need to integrate the VTOL propulsion System, The propeller Size is approximately 1.778m dia, where the radius is 0.889m. why we are concerned about this is we have enough spacing for the propeller that it doesn't hit the fuselage or tail

$$S_h = \frac{V_h * S * C_w}{L_h} = \frac{1.1 * 7.5 * 0.75}{3.85} \approx 1.60m^2$$

SPAN of Horizontal Stabilizer:

Span of Horizontal Stabilizer = $\sqrt{S_h * Aspect\ ratio} = \sqrt{1.60 * 7} \approx 3.35m$

Where, Aspect Ratio of Horizontal Stabilizer is typically, 3 to 7. The Aspect ratio considered is 7**.**

Chord Length $= \frac{S_h}{HT_{span}} = \frac{1.60}{3.35} \approx 0.47m$

6.5.2 Vertical Stabilizer Sizing

In a twin boom configuration, the vertical stabilizers are mounted on the booms. Each vertical stabilizer must provide sufficient yaw stability.

Formula:

The vertical tail volume coefficient (V_v) is given by:

$$V_v = \frac{S_v * L_v}{S * Wingspan}$$

Where:

- S_v = Total vertical stabilizer area (for both booms).
- S = Wing Surface Area
- L_V = Tail arm (same as L_h for twin booms).

For UAVs, V_v typically ranges from 0.02 to 0.05**,** by using mid value of 0.04

$$S_v = \frac{V_v * Wingspan * S}{L_v} = \frac{0.04 * 10 * 7.5}{3.85} \approx 0.779m^2$$

Area per Vertical Stabilizer:

Since there are two vertical stabilizers (one on each boom):

$$S_{v,per\ boom} = \frac{S_v}{2} = \frac{0.779}{2} \approx 0.390m^2$$

SPAN of Vertical Stabilizer:

Span of Vertical Stabilizer = $\sqrt{S_{v,perboom} * Aspect\ ratio} = \sqrt{0.390 * 2} \approx 0.883m$

Here, Aspect Ratio of Vertical Stabilizer is typically, 1.5 to 2.5. So, the AR assumed is 2**.**

Chord Length $= \frac{S_{v,per\ boom}}{VT_{span}} = \frac{0.390}{0.883} \approx 0.441m$

Acceleron Aerospace Journal || AAJ.11.2106-2557
Volume 5, Issue 4, pp (1477-1515)
E-ISSN- 2583-9942
https://dx.doi.org/10.61359/11.2106-2557

7. Propulsion System Selection

Selecting a propulsion system (engine) for the aircraft involves calculating the power required for various flight conditions (e.g., cruise, climb, take-off) and then choosing an engine that can meet or exceed those requirements. Step by step calculations are done to find the required power

7.1 Power Required

The power Required During Cruise and Climb will be calculated. Based on this calculation the Peak Power will be identified which will include a safety margin.

7.1.1 Power Cruise

The power required for level flight is determined by the drag force and the aircraft's velocity. The formula for power required (P_{cruise}) is:

$$P_{cruise} = \frac{D * V}{\eta}$$

Where:

- $D =$ total drag force (in Newtons),
- $V =$ velocity (in meters per second).
- $\eta =$ Propulsion Efficiency

7.1.1.1 Drag Force:

The total drag force is the sum of parasite drag and induced drag:

$$D = \frac{1}{2} * \rho * V^2 * S * C_D$$

Where:

- $\rho =$ air density (0.589 kg/m³ at 7000m AMSL),
- $V =$ velocity (45 m/s),
- $S =$ wing area (7.5 m²)
- $C_D =$ total drag coefficient.

The total drag coefficient (C_D) is the sum of the parasite drag coefficient (C_{D0}) and the induced drag coefficient (C_{Di}):

$$C_D = C_{D0} + C_{Di}$$

Parasite Drag (C_{D0}): This is the drag due to the aircraft's shape and surface roughness. With OpenVSP software, a basic model was created, and the Parasitic drag was roughly estimated. The estimated Parasite drag was 0.07866.

Figure 19 - Parasite Drag Estimation - OpenVSP

Induced Drag (C_{Di}): This is the drag due to lift and is calculated as:

$C_{Di} = \frac{C_l^2}{\pi * e * AR}$

Where:

- C_l = lift coefficient,
- e = Oswald efficiency factor (typically 0.8 to 0.9 for a well-designed aircraft),
- AR = aspect ratio of the wing.

7.1.1.2 Lift Coefficient (C_l):

The lift coefficient is already determined, where the

$$C_l = 1.3675$$

1. Calculate C_{Di}

$C_{Di} = \frac{1.3675^2}{\pi * 0.80 * 13.33} \approx 0.05581$

2. Calculate C_D

$$C_D = 0.07866 + 0.0558 \approx 0.13447$$

3. Calculate drag force (D)

$$D = \frac{1}{2} * 0.589 * 45^2 * 7.5 * 0.13447 \approx 601.44N$$

4. Power Required:

$$P_{cruise} = 601.44 * 45 = 27{,}065\,W$$

We have ignored the Propeller efficiency to cross verify if the power required derived here matches with the Constraint analysis

- Thrust, $T_{req} = \left(\frac{T}{W}\right) \times W = 0.0917 \times 6{,}376.5\,N = 584.6\,N$
- Thrust Power, $P_{thrust} = T_{req} \times V = 584.6\,N \times 45\frac{m}{s} = 26{,}307W$
  - The difference is only 648 W, which is about a 2% discrepancy.
  - The tiny 2% difference is negligible in aircraft design and can be attributed to:
    - Rounding in intermediate steps (e.g., using 9.81 for g, or the T/W ratio).
    - Slightly different assumptions in the two analyses (e.g., the exact air density used at 7000m, or minor variations in the drag polar

5. Power Required with real time Propeller Efficiency

$$P_{cruise} = \frac{601.44 * 45}{0.75} = 36{,}086W$$

($\eta = 0.75$, Assumed Propulsion efficiency.)

So, the Power Required During Cruise is **36,086 kW.**

The power required during Cruise with Various Airspeed has been plotted Below.

7.1.2 Power Climb

To calculate the power required during climb, we need to account for the additional energy required to overcome gravity while maintaining the climb speed.

Acceleron Aerospace Journal || AAJ.11.2106-2557
Volume 5, Issue 4, pp (1477-1515)
E-ISSN- 2583-9942
https://dx.doi.org/10.61359/11.2106-2557

The Climb Angle has been already calculated and its,

$$\alpha_{eff} = 5.48°$$

7.1.2.1 Thrust Required for Climb ($\mathbf{T_{climb}}$)

The thrust required during climb is the sum of:

1. Thrust to overcome drag (D_{climb}).
2. Thrust to overcome the component of weight acting along the flight path.

The total thrust required is:

$$T_{climb} = D_{climb} + W * \sin\theta$$

The $\sin\theta$, has been already calculated in the Climb Analysis (5.3.2) and the value is

$$sin\,\theta = sin(5.48) = 0.0932$$

7.1.2.1.1 Calculate Drag Force During Climb ($\boldsymbol{D_{climb}}$):

The drag force during climb will be slightly higher than during cruise due to the increased angle of attack. We can approximate it as

$$D_{climb} \approx D_{cruise} * (1 + k * \sin\theta)$$

Where k is a factor accounting for the increase in drag due to climb (assume for k=1.2, as we need to take the VTOL Propulsion system into account, which will be forming more drag than a simple fixed wing Aircraft).

From the previous calculation, $D_{climb} \approx 599N$, So,

$$D_{climb} = 601.44 * (1 + 1.2 * 0.0932) = 601.44 * 1.11184 = 668.76N$$

7.1.2.1.2 Thrust to Overcome Weight Component:

The component of weight acting along the flight path is

$$W * sin\,\theta = MTOW * g * sin\,\theta$$
$$W * sin\,\theta = 650 * 9.81 * 0.0932$$

$$W * sin\,\theta = 594.29$$

7.1.2.1.3 Total Thrust required for Climb:

$$T_{climb} = D_{climb} + W * \sin\theta$$

$$T_{climb} = 594 + 668.76 \approx 1{,}263N$$

7.1.2.1.4 Power Required During Climb ($\boldsymbol{P_{climb}}$)

$$P_{climb} = \frac{T_{climb} * V}{\eta} = \frac{1263 * 45}{0.75} \approx 75{,}783W$$

7.1.2.1.5 Adjusted Peak Power Requirement

$$P_{peak} = P_{climb} * (1 + Safty\ Margin)$$

Assuming a **10% safety margin**:

$$P_{peak} = 75{,}783 * (1 + 0.10) \approx 83{,}361W$$

A python code was developed to do the power calculations and cross verify them with the manual calculations which were done above.

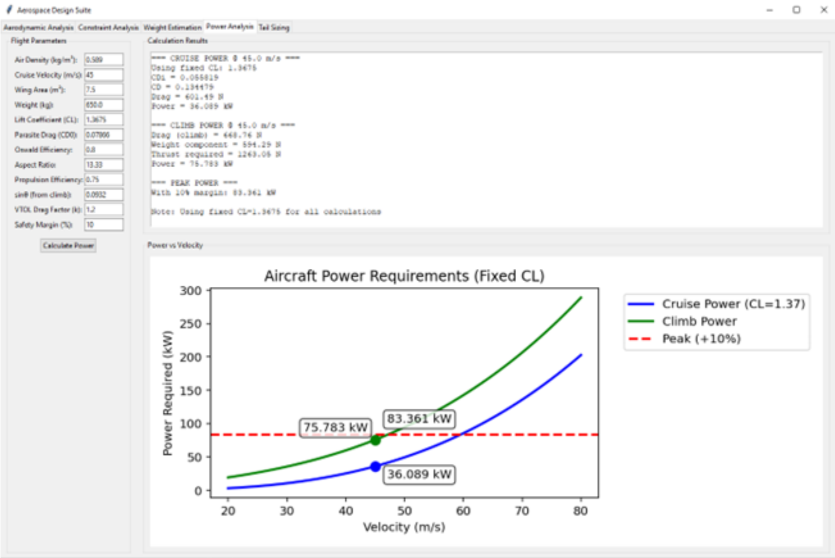

Figure 20 - Aircraft Power Requirement Analysis

7.2 Engine Selection

7.2.1 Engine

Based on the Peak Power obtained, the ROTAX 914 UL | F Engine has been selected. 914 UL | F is one of the industry standard Engine, which has the required Quality and power, and it performs the best in class.

Specifications:

1. Max Power: 115 HP (85.75 kW)
2. Max Torque: 144 Nm
3. Max RPM: 5800
4. Displacement: 1211 CC
5. SFC: 0.28 Kg/kW-hr (This Matches with the Assumed SFC which was taken into consideration during the Fuel Weight Fraction Calculation)

Figure 5- ROTAX 914 UL | F Engine

7.2.2 Propeller

Based on the Engine selected, we have chosen the propellers. Propellers are recommended by the Engine OEM. As the engine is mounted on the backside of the fuselage, the propellers chosen will be of pusher configuration

- AP332S - WWL66Z
- Sensenich Propeller - 2A0R5L69EN

Acceleron Aerospace Journal || AAJ.11.2106-2557
Volume 5, Issue 4, pp (1477-1515)
E-ISSN- 2583-9942
https://dx.doi.org/10.61359/11.2106-2557

Figure 22 - Tri Blade Propellers

7.3 VTOL Power Required

The power required for the VTOL hover phase is calculated using momentum theory. To ensure robust performance and adequate control authority during take-off and landing, especially at high altitudes, a thrust-to-weight ratio (T/W) of 1.15 is specified for the VTOL system. This is applied to the Maximum Take-Off Weight (MTOW) of 650 kg.

$$\boldsymbol{Design\,Thrust}: T_{req} = 1.15 * MTOW = 1.15 * 650 \approx 750\,kg$$

Based on the above Design thrust, The Power required to achieve this thrust is calculated using the Momentum Theory

$$P_{hover} = \frac{(M * g)^{\frac{3}{2}}}{FoM * \sqrt{(2\rho\pi N_r)} * r_{prop}} = \frac{(750 * 9.81)^{\frac{3}{2}}}{0.7 * \sqrt{(2 * 0.589 * \pi * 8)} * 0.89} \approx 1{,}86{,}219W$$

Where:

- $M =$ Mass,
- $FoM = Figure\ of\ Merit$
- $\rho = Density$
- $N_r = Number\ of\ Rotors$
- $r_{prop} = Prop\ radius\ in\ meters.$

Here, the M= 750kg because we consider the T:W ratio to be 1.15:1 and the propeller radius to be 0.89m (70 inches diameter). This is a Coaxial layout, so 8 rotors are considered, and generally for UAVs, the FoM is between 0.6 to 0.8, so a mid-value of 0.7 is considered. The Take-off can be anywhere between 0 – 7000m AMSL, so to ensure the required power is always there, the Air density at 7000m AMSL is considered.

As it is a coaxial layout, a performance loss of 25% is considered.

$$P_{hover,final} = P_{hover} * 1.25 = 1{,}86{,}219 * 1.25 \approx 2{,}32{,}773\ W$$

To get the Individual Power of each motor we Divide the Hover Power by No of Rotors

$$P_{individual} = \frac{P_{hover,final}}{N_r} = \frac{2{,}32{,}773}{8} \approx 29{,}069\ W$$

7.4 VTOL & Avionics Battery Capacity Estimation

With the Known hover power and the following assumptions, the Battery capacity is easily calculated

Assumptions:

Take-off time: 2 minutes

Landing Time: 2 minutes

Battery Configuration (No. of cells): 30S

Voltage per cell during take-off: 4V

Voltage per cell during landing: 3.3V

7.4.1 Battery Voltage During Take-off and Landing

1. $V_{Take-off} = 30 * 4 = 120V$
2. $V_{Landing} = 30 * 3.3 = 99V$

7.4.2 Energy Required for Take-off and Landing

$$E_{required} = P_{hover} * T = 2{,}32{,}773 * 0.033 \approx 7{,}681Wh$$

The time taken for Take-off and Landing are same, so we need to multiply the Required Energy with 2.

$$E_{propulsion} = 7{,}681 * 2 = 15{,}363Wh$$

7.4.3 Voltage Nominal

Here, $V_{nominal}$ is the average voltage during the flight. We can approximate it as the average of take-off and landing voltages:

$$V_{nominal} = \frac{V_{Take-off} + V_{Landing}}{2} = \frac{120 + 99}{2} = 109.5\,V$$

7.4.4 Avionics energy

The avionics power is assumed as 30 Ah. To convert this to energy, it is multiplied by the nominal voltage of the battery.

$$E_{avionics} = 30Ah * 109.5V = 3{,}285Wh$$

7.4.5 Battery Capacity

The battery capacity in Ampere-hours (Ah) is given by:

$$C_{batt} = \frac{E_{propulsion} + E_{avionics}}{V_{nominal}}$$

$$C_{batt} = \frac{18{,}648}{109.5} \approx 170Ah$$

Key Notes: When the aircraft is in long endurance mission, the Avionics power will be taken from the engine using an alternator, which will eliminate the fear about the instrument's endurance.

7.4.6 Battery Weight Estimation

The total weight of the battery is given by:

$$W_{batt} = \frac{E_{total}}{E_{density}} = \frac{18{,}648}{400} \approx 46.62kg$$

Where, the assumed battery energy density is 400Wh/Kg.

Acceleron Aerospace Journal || AAJ.11.2106-2557
Volume 5, Issue 4, pp (1477-1515)
E-ISSN- 2583-9942
https://dx.doi.org/10.61359/11.2106-2557

7.5 VTOL Propulsion System

Based on the calculations, the REB 30 ELECTRIC MOTOR from MGMCompro has been chosen which can deliver up to 30kW as continuous power. Along with this, HBCI 320120-3 ESC, The Mejzlik 70x24 Propeller and A Customised Battery pack has been chosen which matches the propulsion requirement

Motor:

Specifications of the Motor:

- Max Power: 40kW
- Max Cont. Power: 30kW
- Max Torque: 150Nm
- Max RPM: 4000
- Max Voltage: 60-800V

Figure 23 - MGMCompro REB 30 Electric Motor

Electronic Speed Controller:

Specifications of the Controller:

- Max Cont. Current: 320Amps
- Max Cont. Power: 38kW
- Peak Current: 600Amps
- Max Voltage: 16-120V\
- CAN protocol Supported
- Inbuild data logging

Figure 24 - HBCi ESC

Propeller:

Based on the selected motor and from the recommendation of OEM, the Following propeller has been chosen - Mejzlik 70x24

Figure 25 - Mejzlik Propeller

Battery Pack:

Based on the calculations and motor selected, MGM Customized Battery has been chosen.

The battery has the following spec:

- Max – C Rating: 60C
- Energy Density – 400Wh/kg
- Max Voltage :800 (Required Voltage: 120) (30S Battery pack)
- BMS Included

Figure 26 - MGMCompro Customized Battery Pack

8. Aircraft Design and Weight Distribution

8.1 Weight Distribution

Table 8 - Weight Distribution for Sub-systems

S.no	System/Sub-System	Qty of Sub-system in AC	Individual Weight of the Sub-system (Kg)	Total Weight (Kg)
1	Engine	1	64	64
2	Fixed wing Propeller	1	11.3	11.3
3	VTOL Motor	8	8.15	65.2
4	ESC	8	1.035	8.28
5	VTOL Propeller	8	0.7	5.6
6	Battery	1	46.62	46.62
7	Other Avionics and Harnesses (Assumed)	1	20	20
			Total Weight	**221**

From 4.5 Final Weight Distribution:

Finally, The Empty Weight Estimated is 352.81kg, So, if we subtract the total sub system weight, the Actual weight allowance for the structure is estimated

Acceleron Aerospace Journal || AAJ.11.2106-2557
Volume 5, Issue 4, pp (1477-1515)
E-ISSN- 2583-9942
https://dx.doi.org/10.61359/11.2106-2557

$$Structure\ Weight = W_{empty} - W_{Sub-system}$$

$$W_{Structure} = 352.81 - 213.6 = 139.21\ Kg$$

The final estimated weight is on the table below

Table 9 - Final Weight Estimation with Sub-systems

Weights	Value
$W_{Structure}$	131.83 Kg
$W_{Sub-system}$	221 Kg
$W_{payload}$	112 Kg
W_{Fuel}	185.17 Kg
W_{total}	650kg

8.2 Aircraft Design

With the Above design calculations that were made, the aircraft was designed using the OpenVSP aero Software.

To Differentiate and see if the performance changes with various Fuselage Length, Tail Arm length and the associated design parameters, three different Sizes were done, and the Analysis was carried out. The wing Parameters were not disturbed as the wing analysis was already performed in XFLR5 and found satisfactory.

Table 10 - Aircraft Design parameters with 3 different tail arm length

Design 1 with Tail Arm 3.5m	Design 2 with Tail Arm 3.85m	Design 3 with Tail Arm 4.2m
Fuselage Length: 5 m	Fuselage Length: 5.5 m	Fuselage Length: 6 m
Fuselage Diameter: 0.6m	Fuselage Diameter: 0.6m	Fuselage Diameter: 0.6m
Wingspan: 10m	Wingspan: 10m	Wingspan: 10m
MAC: 0.75m	MAC: 0.75m	MAC: 0.75m
Wing AR: 13.33	Wing AR: 13.33	Wing AR: 13.33
Tail arm Length: 3.5m	Tail arm Length: 3.85m	Tail arm Length: 4.2m
HT Span: 3.51m	HT Span: 3.35m	HT Span: 3.21m
HT Chord: 0.50m	HT Chord: 0.49m	HT Chord: 0.45m
LHS VT Span: 0.926m	LHS VT Span: 0.883m	LHS VT Span: 0.845m
RHS VT Span: 0.926m	RHS VT Span: 0.883m	RHS VT Span: 0.845m
LSH VT Chord: 0.463m	LSH VT Chord: 0.441m	LSH VT Chord: 0.423m
RHS VT Chord: 0.463m	RHS VT Chord: 0.441m	RHS VT Chord: 0.423m
Boom Length: 5.2m	Boom Length: 5.8m	Boom Length: 6.2m
Boom Diameter: 0.1m	Boom Diameter: 0.1m	Boom Diameter: 0.1m

Analysis:

After designing the aircraft, it was subjected to the VSPAERO Analysis tool, where the following boundary conditions were defined:

1. The Airspeed: 45m/s
2. Altitude: 7000m AMSL
3. Density: 0.589
4. RPM of the Fixed wing Propeller during Cruise: 3000RPM
5. Angle of Attack Range: -15 to 20 Deg

Post processing, Following were the Results obtained:

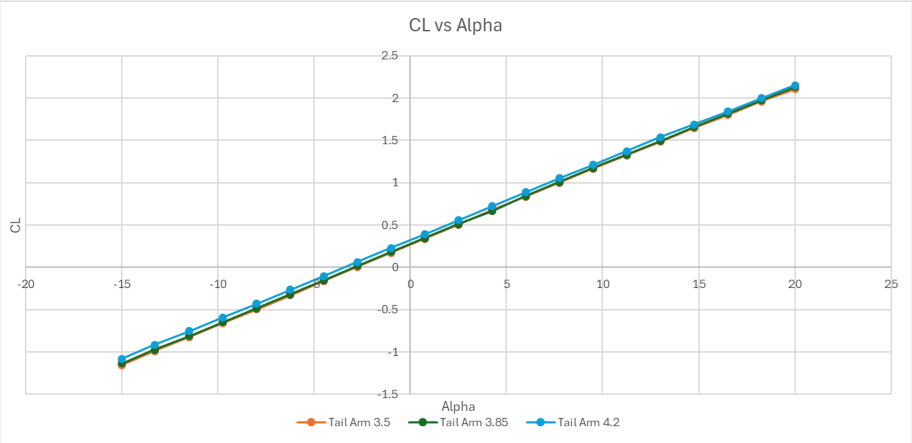

Figure 6 - CL vs Alpha

1. Linear Lift Curve (Good Lift Generation)

- The CL vs. Alpha plot shows a smooth, linear increase in lift coefficient (CL) with Alpha, which is a sign of well-behaved aerodynamic performance.
- This indicates that the wing is efficiently generating lift within the analysed range.

2. Zero-Lift Angle of Attack ($\alpha_0 L$)

- The zero-lift AoA (where CL = 0) appears to be around -2° to -3°.
- This suggests that the airfoil has a slightly cambered profile, which is typical for most efficient wings used in UAVs and aircraft. The slope of the curve (dCL/dα) appears to be nearly constant, meaning your wing is providing predictable lift increments with AoA changes

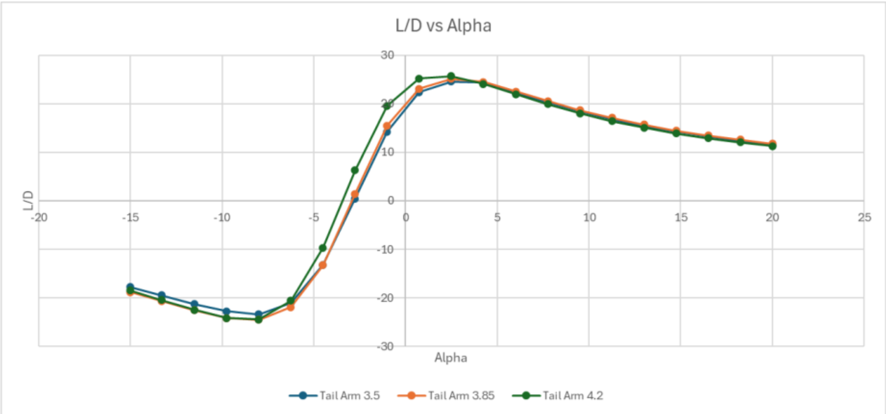

Figure 7 - L/D vs Alpha

Acceleron Aerospace Journal || AAJ.11.2106-2557
Volume 5, Issue 4, pp (1477-1515)
E-ISSN- 2583-9942
https://dx.doi.org/10.61359/11.2106-2557

1. Expected Trend Observed

- L/D increases from negative values at low AoA, peaks around 3° AoA (~25 L/D), and then declines due to drag rise.
- The curve suggests good aerodynamic efficiency with expected post-stall behavior.

2. Peak L/D Optimization

- The highest efficiency occurs at 0° to 5° AoA, so we need to ensure cruise AoA is close to this for fuel efficiency and endurance.
- If cruise happens at a lower L/D, airfoil or trim adjustments may be needed.

3. Drag and Stall Considerations

- Sharp L/D decline after the peak suggests flow separation or increased drag, possibly indicating early stall onset.

4. Mission-Specific Adjustments

- If this is a long-endurance UAV, maintaining flight near peak L/D AoA is ideal.

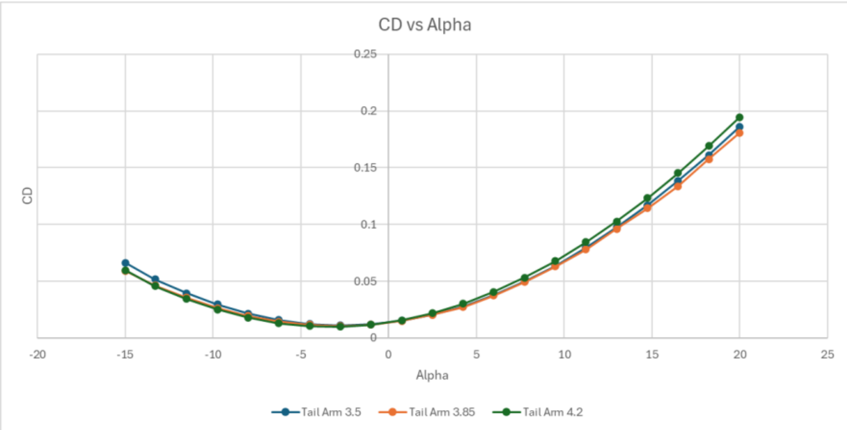

Figure 8 - CD vs Alpha

1. Expected Drag Curve Shape

- Drag (CDtot) is lowest near 0° AoA and increases symmetrically for positive and negative angles.
- The curve follows the expected parabolic trend due to induced drag dominance at high AoA.

2. Minimum Drag and Efficiency

- The minimum drag occurs around -2° to 0° AoA, which aligns with most efficient cruise angles.
- If cruise AoA is higher, airfoil or trim adjustments may help to reduce drag.
- Post-Stall Drag Rise
- The sharp increase beyond 10° AoA suggests stall onset, causing separation-induced drag.
- This confirms that maintaining flight below 10° AoA is ideal for efficiency.

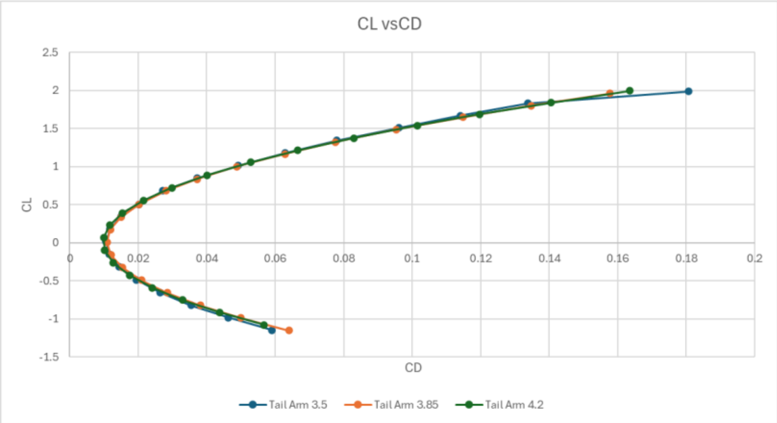

Figure 9 - CL/CD vs Alpha

Shape: The curve is well-formed, showing an expected increase in Cd as Cl increases, which is characteristic of aerodynamic efficiency.
Symmetry: The negative Cl values indicate that the airfoil is analyzed in both positive and negative AoA regions, which is useful for stability analysis.
Drag Values: The Cd values are in a reasonable range (0.02 - 0.18), aligning with aerodynamic expectations for typical airfoils.

With the Above graphs and data, it's found that the Aerodynamic Efficiency is aircraft is well performing.

9. Stability and Control

The UAV movement has six degrees of freedom, which has three translational and three rotational movements which are intended to be important for manoeuvring stability.

- The Longitudinal stability is directly associated with pitching motion of the UAV.
- The Lateral Stability is Directly associated with the rolling motion of the UAV.
- The Directional Stability is directly associated with the yawing motion of the UAV.

9.1 Longitudinal Stability

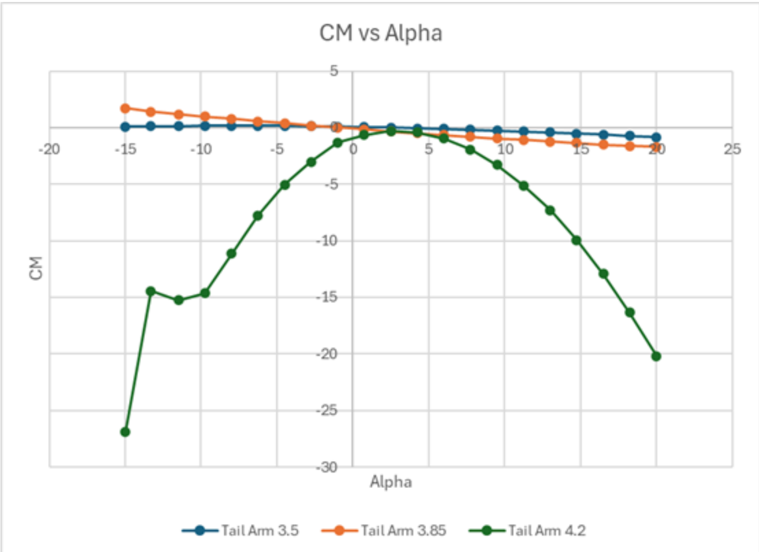

Figure 10 - CM vs Alpha

Here, it is seen that the Pitching moment of the design with Tail Arm 4.2m is unstable and its Shows a strong nonlinear trend, with CM changing significantly as the AoA increases. At negative angles, a sudden increase in pitching moment is observed, possibly indicating flow separation or instability at certain negative alpha and at higher angles of attack, the curve becomes steeply negative, which suggests a high stabilizing moment but might indicate excessive nose-down pitching.

Considering this we can eliminate the Tail Amr length of 4.2m and we will plot Tail Arm of length 3.85m and 3.5m to see the stability

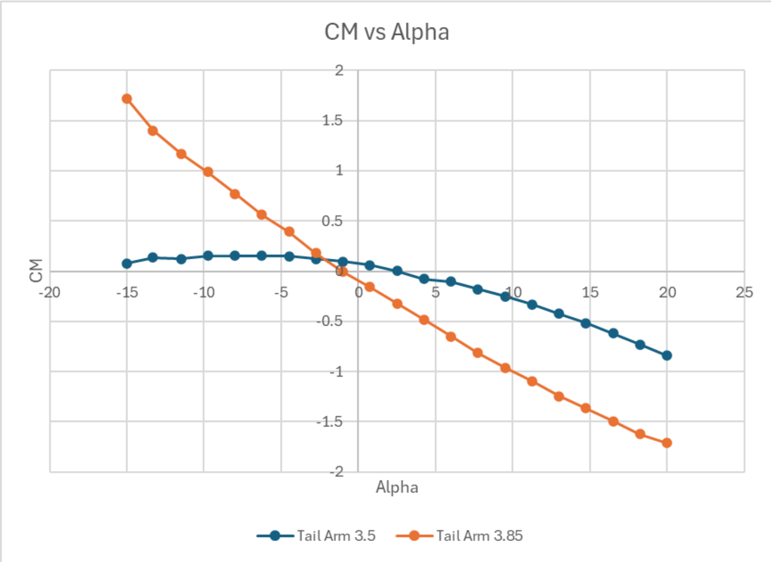

Figure 11 - CM vs Alpha without Tailarm 4.2m

9.1.1 Analysis of Updated CM vs Alpha Plot

This updated graph compares the moment coefficient (CM) against the angle of attack (AoA) for tail arm lengths of 3.5 and 3.85.

1. **Tail Arm 3.5 (Blue Curve)**
   - CM remains nearly constant across all angles of attack, indicating low pitch control effectiveness.
   - A flat curve suggests neutral stability, meaning the aircraft might not naturally return to its trimmed angle after a disturbance.
2. **Tail Arm 3.85 (Orange Curve)**
   - Shows a linearly decreasing trend, which is expected for a stable aircraft.
   - The negative slope suggests that increasing α\alphaα results in a restoring moment, which is essential for static stability.
   - The point where CM=0 is the trimmed angle of attack.

Observations & Recommendations

Tail Arm 3.85 is the better choice as it provides a restoring moment for stability.

If additional stability is required, increasing the tail arm slightly beyond 3.85 could be considered, but avoiding excessive values to prevent overcorrection.

9.2 Lateral Stability

Based on the pervious analysis, the Lateral Stability was analysed only for the Design of Tail Arm Length of 3.85m

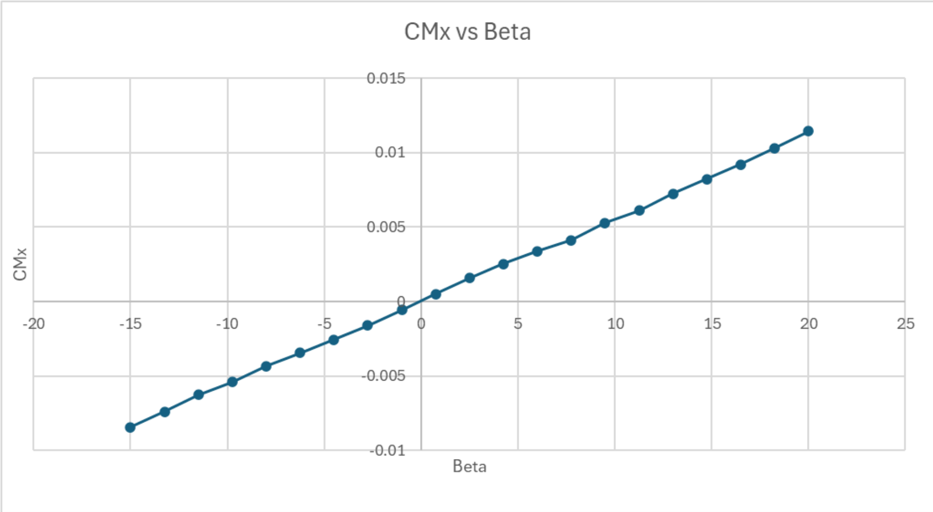

Figure 12 - CMx vs Beta

1. **Linear Trend**: The CMx vs Beta graph shows a near-linear trend, increasing with Beta. This indicates a steady roll moment variation with sideslip angle.
2. **Stable Roll Characteristics**: The gradual increase suggests predictable and stable rolling behavior, essential for maintaining lateral stability.
3. **Possible Wing Dihedral Effect**: The trend suggests a positive dihedral effect, where roll moment increases symmetrically with sideslip.

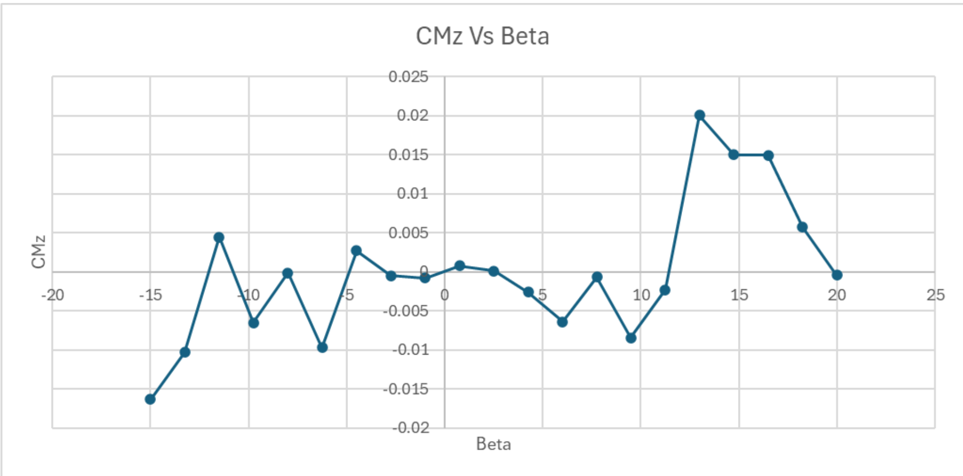

Figure 13 - CMz vs Beta

1. **Irregular Variation**: Unlike CMx, CMz vs Beta has noticeable fluctuations, indicating oscillatory yawing moments with sideslip.
2. **Yaw Instability**: The sharp peaks suggest instability or unsteady aerodynamic effects, possibly due to asymmetric flow separations.
3. **Potential Rudder or Fuselage Impact**: The fluctuations might be due to rudder effectiveness variations or fuselage vortex interactions.

To compensate the same, multiple design iterations were carried out with the Sizing of the rudder, but they weren't fruitful.

9.2.1 Airfoil Change (NACA0012 to NACA0020)

The substitution of the vertical stabilizer airfoil from NACA 0012 to NACA 0020 was crucial for achieving directional stability. The primary reason is the effect of airfoil thickness on vortex shedding and flow separation. The NACA 0012, being thinner, is more prone to early flow separation at moderate to high sideslip angles (β). This separated flow is highly unsteady and leads to asymmetric vortex shedding, which manifests as the irregular and unpredictable yawing moments (fluctuations in CMz) observed in the initial analysis.

Acceleron Aerospace Journal || AAJ.11.2106-2557
Volume 5, Issue 4, pp (1477-1515)
E-ISSN- 2583-9942
https://dx.doi.org/10.61359/11.2106-2557

The NACA 0020, with its greater 20% thickness, has a more gradual pressure recovery gradient. This delays the onset of significant flow separation to higher angles of attack. For the vertical stabilizer, this translates to a more attached and predictable flow field over a wider range of sideslip angles. The result is a smoother, linear variation of the yawing moment coefficient (CMz) with β, as seen in Figure 35, which is a hallmark of stable and controllable directional characteristics. Finally, the Vertical Stabiliser Aerofoil was changed NACA0012 to NACA 0020, with this change the results were as consistent and the same has been plotted below.

Analysis of CMz vs Beta(NACA 0020 Airfoil):

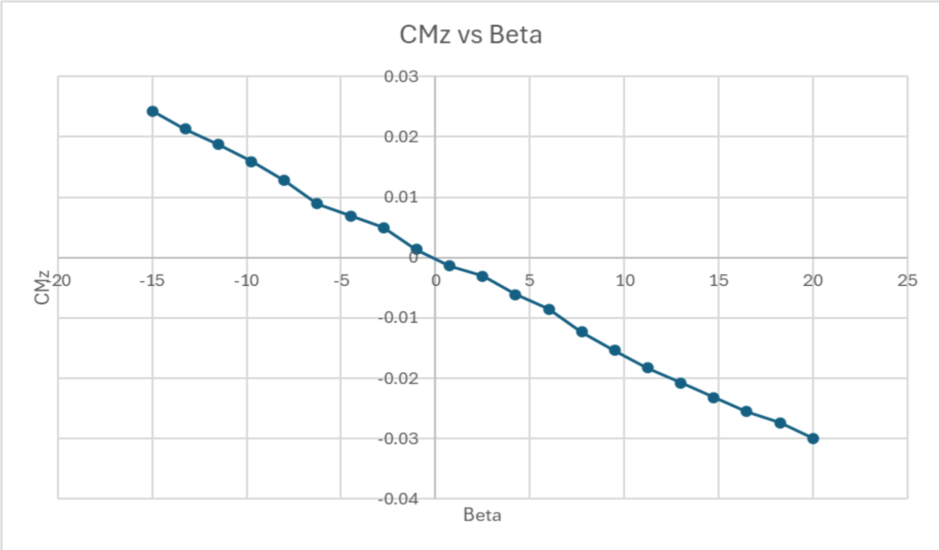

Figure 14 - CMz vs Beta (NACA 0020)

1. **Linear Behavior**: The moment coefficient (CMz) decreases steadily as the sideslip angle (Beta) increases. This suggests predictable yaw stability characteristics.
2. **Yaw Stability**: A negative slope means that as the aircraft yaws (experiences sideslip), the restoring moment acts in the opposite direction, helping bring the aircraft back to its original orientation. This is a sign of a stable design.
3. **Zero Crossing at Beta = 0**: The graph passes through the origin, indicating symmetry in yaw. There is no inherent yawing moment when the aircraft is in a zero-sideslip condition.

The 3D view and Isometric view of the aircraft.

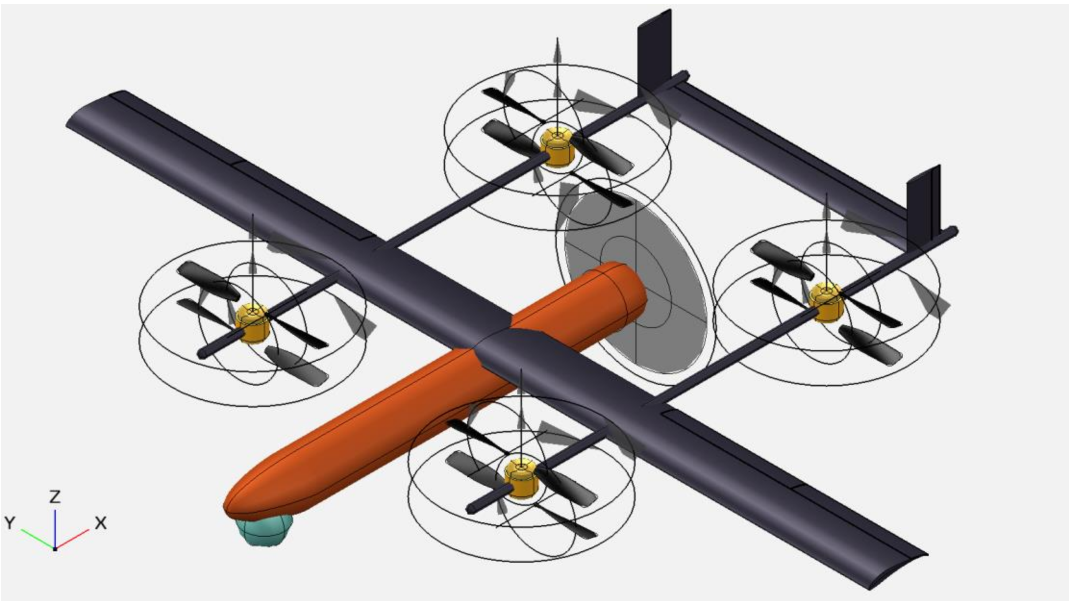

Figure 15 – Aircraft Design in OpenVSP

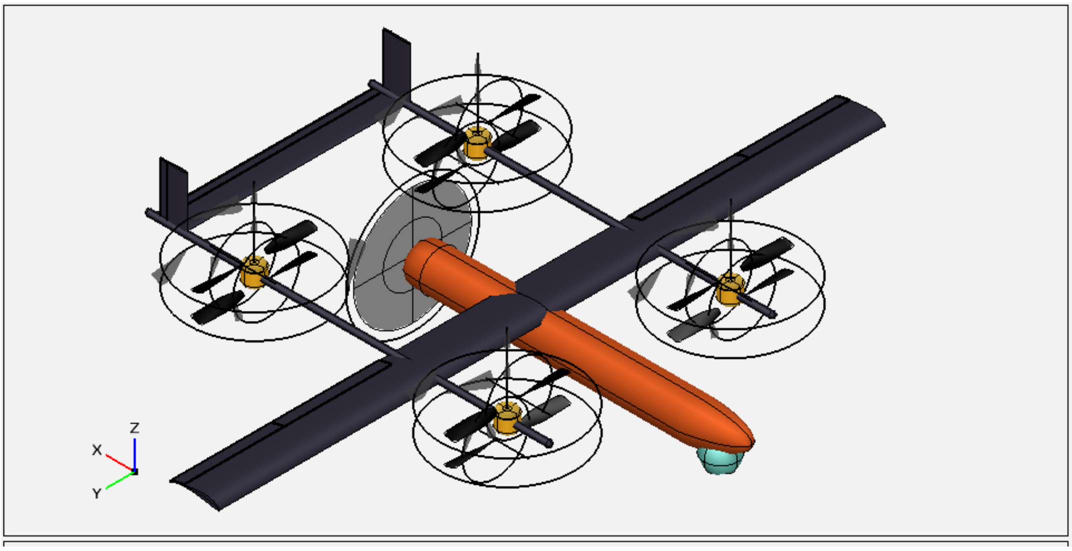

Figure 16 - Right ISO View

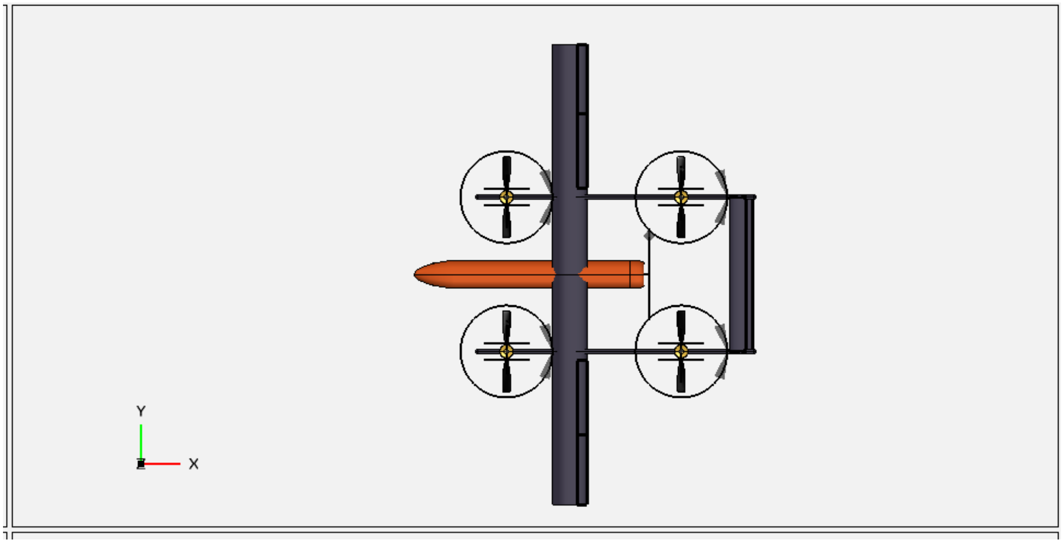

Figure 17 - Top View

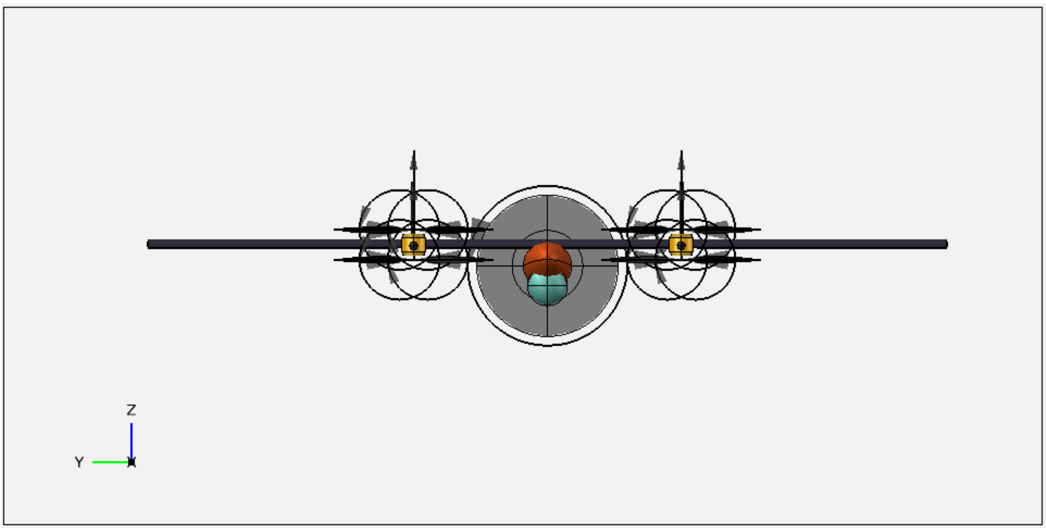

Figure 18 - Front View

Acceleron Aerospace Journal || AAJ.11.2106-2557
Volume 5, Issue 4, pp (1477-1515)
E-ISSN- 2583-9942
https://dx.doi.org/10.61359/11.2106-2557

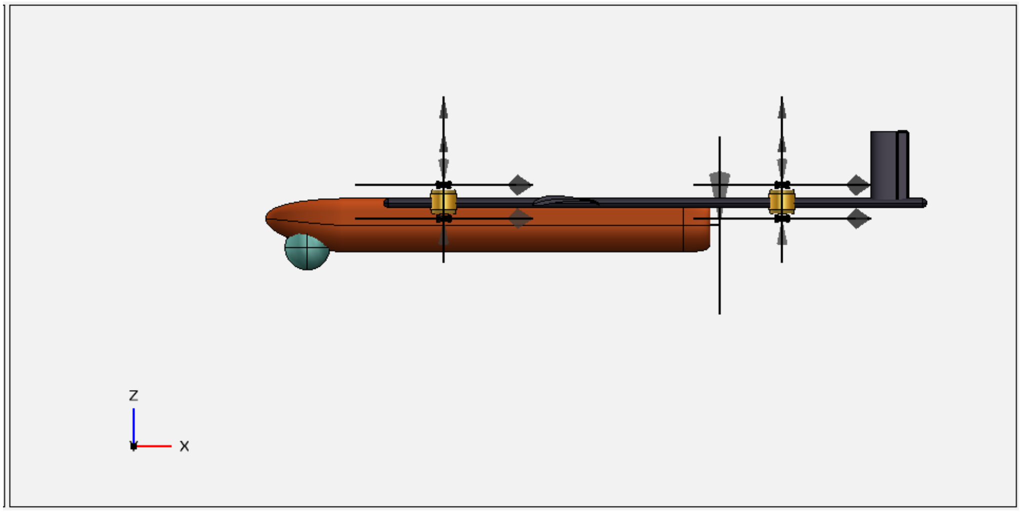

Figure 19 - Side View

10. Assumptions and Limitations

This conceptual design study is based on a set of necessary assumptions and is subject to certain limitations, which should be addressed in subsequent detailed design phases.

10.1 Key Assumptions

Weight Estimation: The initial weight breakdown relied heavily on empirical relations from historical data (Raymer). The actual weight of the integrated structure, especially the novel twin-boom with VTOL integration, may vary.

Aerodynamic Coefficients: The Oswald efficiency factor ($e=0.8$), zero-lift drag coefficient ($CD0$), and propeller efficiency ($\eta=0.75$) were assumed based on typical values for similar aircraft. These require empirical validation.

Stability Analysis: The VSPAERO analysis used is an inviscid panel method. While excellent for initial stability trends, it does not fully capture viscous effects like boundary layer separation, which can affect high-angle-of-attack and stall predictions.

VTOL Transition: The analysis treated the VTOL and fixed-wing flight phases somewhat independently. The complex, dynamic transition phase between hover and cruise was not modeled in detail and is a critical area for future study.

Environmental Conditions: The analysis assumed standard atmospheric conditions. The impact of severe turbulence, icing, or heavy precipitation on performance and stability was not considered.

10.2 Study Limitations

Computational Fidelity: The aerodynamic and stability analyses were conducted using low- to mid-fidelity tools (XFLR5, OpenVSP). Higher-fidelity CFD and FEA are required to resolve complex flow phenomena and structural stresses accurately.

Control System Design: This study focused on the inherent stability of the airframe. The design of the automatic flight control system (AFCS) required to manage the VTOL transition and overall flight stability was beyond its scope.

Manufacturing Considerations: The design has not yet been optimized for manufacturability, and material selection was preliminary. Factors such as cost, assembly, and maintenance were not primary drivers in this phase."

10.2 Study Limitations

Computational Fidelity: The aerodynamic and stability analyses were conducted using low- to mid-fidelity tools (XFLR5, OpenVSP). Higher-fidelity CFD and FEA are required to resolve complex flow phenomena and structural stresses accurately.

Control System Design: This study focused on the inherent stability of the airframe. The design of the automatic flight control system (AFCS) required to manage the VTOL transition and overall flight stability was beyond its scope.

Manufacturing Considerations: The design has not yet been optimized for manufacturability, and material selection was preliminary. Factors such as cost, assembly, and maintenance were not primary drivers in this phase."

11. Conclusion

In this study, we have systematically designed and analysed a 650kg VTOL UAV, focusing on aerodynamics, propulsion, and structural efficiency. The proposed design integrates both fixed-wing and VTOL capabilities, ensuring optimal endurance and operational versatility. Through detailed weight estimations and propulsion system selection, we have validated the feasibility of achieving the desired performance metrics. Computational simulations and empirical calculations indicate that the UAV meets stability and control requirements across various flight phases. Additionally, our findings highlight the importance of airfoil selection and power optimization in enhancing endurance. The thrust-to-weight ratio and energy efficiency were carefully balanced to ensure effective vertical and horizontal transitions. The insights from this conceptual design provide a robust foundation for the next stages of development, as outlined in the future work section

12. Future Scope of Work

While this study establishes a feasible conceptual design, the following steps are recommended to advance the design towards a prototype and flight testing:

Detailed CAD and Structural Analysis: Develop a high-fidelity 3D CAD model to perform Finite Element Analysis (FEA). This will validate structural integrity under critical loads from VTOL, cruise, and gust conditions, and enable detailed weight optimization.

High-Fidelity CFD Analysis: Conduct Computational Fluid Dynamics (RANS/LES) simulations to accurately model the complex flow interactions during the VTOL-to-cruise transition phase, assess propeller-wing interactions, and refine drag predictions.

Flight Dynamics and Control Law Synthesis: Develop a non-linear 6-Degree-of-Freedom (6-DoF) flight dynamics model. This model is essential for designing and simulating the flight control system, especially for the autonomous transition phase between hover and forward flight.

Prototyping and Wind Tunnel Testing: Construct a sub-scale prototype for wind tunnel testing to empirically validate aerodynamic performance and stability derivatives, particularly for the hybrid VTOL-fixed wing configuration.

Systems Engineering Integration: Perform detailed design of subsystems including the fuel system, landing gear (for emergency scenarios), thermal management for batteries and motors, and the communication/data-link architecture.

13. Data Availability Statement

The data presented in this study are available upon request from the corresponding author. The data is not publicly available due to ongoing research and development activities associated with the presented prototype.

14. References

[1] Varsha, N., & Somashekar, V. (2018). Conceptual design of high performance unmanned aerial vehicle. IOP Conference Series: Materials Science and Engineering, 376, 012056. https://doi.org/ 10.1088/1757-899X/376/1/012056.

[2] Jenkinson, L., & Marchman, J. (2003). Aircraft design projects. Elsevier. https://doi.org/10.1016/B978-0-7506-5772-3.X5000-5.

[3] Ramer, D. P. (1992). Aircraft design: A conceptual approach. AIAA.

[4] Anderson, J. D. (2011). Aircraft performance and design. Elsevier.

[5] Song, S. (2024). Study on development of aircraft design theory. Proceedings of the 3rd International Conference on Computing Innovation and Applied Physics. https://doi.org/10.54254/2753-8818/13/20240772

[6] Spada, V. (2019). Conceptual design of MALE UAVs (Graduate theses, dissertations, and problem reports No. 7374). West Virginia University.

[7] Lowry, J. T. (1999). Performance of light aircraft. American Institute of Aeronautics and Astronautics.

E-ISSN- 2583-9942
https://dx.doi.org/10.61359/11.2106-2557

[8] Austin, R. (2011). Unmanned aircraft systems: UAVs design, development and deployment. John Wiley & Sons.
[9] McClamroch, N. H. (2011). Steady aircraft flight performance. Princeton University Press.
[10] Weissberg, V., Interator, M., Schwartzberg, A., Gueta, A., Menikes, G., Steinberg, A., Hachman, N., & Gali, S. (1995, May 8–11). High altitude long endurance RPV. 40th International SAMPE Symposium.
[11] Altunok, T. (2010). Development of unmanned aerial vehicles. Science and Technology, 517, 28–31.
[12] Gudmundsson, S. (2013). General aviation aircraft design: Applied methods and procedures. Butterworth-Heinemann.
[13] Stone, R. H., & Clarke, G. (2001). The T-Wing: A VTOL UAV for naval operations. Proceedings of the 20th Bristol International RPV/UAV Systems Conference.
[14] Ohanian, O., et al. (2012). Hybrid VTOL UAV for remote sensing. International Journal of Mechanical, Aerospace, Industrial, Mechatronic and Manufacturing Engineering, 6(10), 2155–2162.
[15] van Blyenburgh, P. (2006). UAV systems: Global review. UAV DACH Symposium, 1–51.
[16] Mueller, T. J. (2004). Aerodynamic measurements at low Reynolds numbers for fixed wing micro-air vehicles. Hessert Center for Aerospace Research, University of Notre Dame, 21, 3–36. http://www.jstor.org/stable/20753438
[17] Phillips, W. F. (2004). Mechanics of flight. John Wiley & Sons.
[18] Leishman, J. G. (2006). Principles of helicopter aerodynamics (2nd ed.). Cambridge University Press.
[19] Hu, Y. X., & Tianyuan, Y. (2008). Aerodynamic/stealthy/structural multidisciplinary design optimization of unmanned combat air vehicle. Chinese Journal of Aeronautics.
[20] Nguyen, N. M. T., et al. (2015, May 18). Aerodynamic analysis of aircraft wing. VNU Journal of Science: Mathematics.
[21] Mueller, T. J., & DeLaurier, J. D. (2003). Aerodynamics of small vehicles. Annual Review of Fluid Mechanics, 35(1), 89–111.
[22] Lee, J. W., Nguyen, N. V., Choi, S. M., Kim, W. S., Jeon, K. S., & Byun, Y. H. (2009). Multidisciplinary unmanned combat air vehicle (UCAV) design optimization using variable complexity modelling. Proceedings of the 9th AIAA Aviation Technology, Integration, and Operations Conference (ATIO), Hilton Head, USA.

15. Conflict of Interest

The author declares no competing conflict of interest.

16. Funding

No funding was issued for this research.